

NASA TECHNICAL NOTE



NASA TN D-4111

c.1

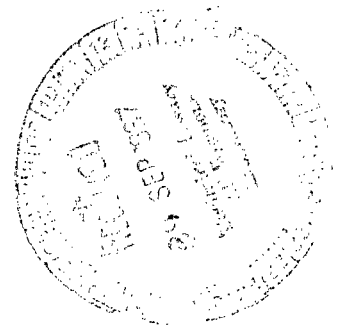
LOAN COPY:  
AIR FORCE  
KIRTLAND AFB



NASA TN D-4111

# HETERODYNE PHASE SHIFTER WITH INDUCTIVE DELAY LINE PICKUP PROVIDES STEPLESS PHASE SHIFT

*by George B. Robinson*  
*Goddard Space Flight Center*  
*Greenbelt, Md.*





HETERODYNE PHASE SHIFTER WITH INDUCTIVE DELAY LINE  
PICKUP PROVIDES STEPLESS PHASE SHIFT

By George B. Robinson

Goddard Space Flight Center  
Greenbelt, Md.

NATIONAL AERONAUTICS AND SPACE ADMINISTRATION

## ABSTRACT

This paper describes the design and construction of a phase shifter which provides calibrated phase shift in a continuous 360-degree range of a sine-wave input signal. The circuit produces phase shift indirectly by introducing a differential phase shift, via calibrated delay lines, to a fixed frequency carrier. The carrier is mixed with the signal to generate a single sideband by means of a balanced mixer followed by a crystal filter. The single sideband is then reheterodyned with the carrier in a second mixer to restore the original frequency. The restored signal phase angle relative to the input signal is equal to the relative phase between the carrier inputs to the first and second mixers. Variable phase output from the calibrated delay lines is obtained by means of an inductive pickup consisting of a wound ferrite toroid with an air gap. The toroid pickup resembles a tape recorder head. This method of delay line pickoff avoids the uncertainty associated with sliding contacts and provides a controlled phase shift characterized by infinite resolution. The phase shifter provides calibrated phase shift without attendant amplitude fluctuation. The measured linearity of phase control in a 360-degree range is  $\pm 2$  degrees. Phase linearity is independent of the input signal frequency. Second harmonic distortion of the output signal is -50 db below the fundamental with a 0.5-volt input signal level. The operating range of the phase shifter is 30 to 200 kHz, with a carrier frequency of 10.580 MHz and 300 to 500 kHz, with a carrier frequency of 10.258 MHz. The circuit, which employs transistors, is temperature-compensated.

## CONTENTS

Abstract . . . . .	ii
INTRODUCTION. . . . .	1
CIRCUIT ANALYSIS . . . . .	1
Input Balanced Mixer Equation . . . . .	3
Single Sideband Filter Equation. . . . .	4
Output Balanced Mixer Equation . . . . .	5
Phase Shifter Output Expression, Normal Operation . . . . .	5
Phase Nonlinearity and Amplitude Variation When Signal Frequency is Below Normal Operating Range . . . . .	7
Phase Nonlinearity Resulting From Improperly Terminated Delay Lines . . . . .	9
Phase Shifter Output for Nonsinusoidal Input . . . . .	11
PHASE SHIFTER DESIGN AND CONSTRUCTION . . . . .	11
Block Diagram. . . . .	11
Input Balanced Mixer . . . . .	16
Input Mixer Carrier Amplifier . . . . .	17
Signal Emitter Follower . . . . .	17
Crystal Filter . . . . .	17
Emitter Follower Filter Driver . . . . .	19
Single Sideband Amplifier . . . . .	19
Output Mixer . . . . .	19
Output Mixer Carrier Amplifier . . . . .	19
Low-Pass Filter and Output Signal Amplifier . . . . .	20
Crystal Oscillator . . . . .	20
Delay Line 2 . . . . .	20
Delay Line 1 . . . . .	23
Differential Amplifier Circuit. . . . .	23
MEASURED PERFORMANCE OF PHASE SHIFTER . . . . .	24
Use of Differential Amplifier for Setting Phase Shifter Zero . . . . .	24
Calibration of Line 2 for Continuous Phase Control, 0- to 360-Degree Range . . . . .	25

CONTENTS (Continued)

Measured Phase Nonlinearity When Line 2 Is Not Terminated in $Z_0$ . . . . .	28
Phase Shifter Operating Range in kHz With a 10.580-MHz Carrier Frequency. . . . .	29
Phase Shifter Signal Amplitude Distortion. . . . .	30
Effects of Ambient Temperature Variation, 65° to 90°F. . . . .	31
Phase Shifter Operating Range in kHz With a 10.258-MHz Carrier Frequency. . . . .	32
CONCLUSIONS. . . . .	32
References . . . . .	33
Appendix A—Partial List of Symbols . . . . .	35
Appendix B—Effect of Lower Sideband on Phase Shifter Output . . . . .	37
Appendix C—Distributed Constant Delay Line With Toroidal Pickup. . . . .	41
Appendix D—Phase Function $\tan^{-1} F \sin W / (1 + F \cos W)$ . . . . .	49

# HETERODYNE PHASE SHIFTER WITH INDUCTIVE DELAY LINE PICKUP PROVIDES STEPLESS PHASE SHIFT

by

George B. Robinson

*Goddard Space Flight Center*

## INTRODUCTION

This paper describes the design and construction of a heterodyne phase shifter which provides a calibrated phase shift in a 0- to 360-degree range of a sine-wave input. Phase shift is produced indirectly by phase-shifting the carrier employed in a double heterodyne process which first converts the input signal to a single sideband by means of a balanced mixer and crystal filter and then reconverts it to the original signal frequency in a second mixer. The carrier is phase-shifted by means of an adjustable delay line with an output obtained from a positioned inductive pickup rather than the usual sliding contact; the inductive pickup offers stepless phase shift with increased reliability. The heterodyne method enables phase shift with constant amplitude over an operating frequency range extending from 30 kHz to 500 kHz, depending on the choice of carrier frequency. Signal bandwidth is 200 kHz for any selected value of carrier frequency.

The paper is organized into three sections. The first section analyzes the heterodyne process and gives the phase shifter output expression. Causes of phase nonlinearity as related to signal frequency and delay-line termination are then considered. This discussion of phase nonlinearity is supplemented by an appendix which also includes an analysis of the inductive pickup. The first section is concluded with an analysis of phase shifter operation with nonsinusoidal inputs. The second section describes the transistorized phase-shifter circuit and includes details for converting a standard adjustable delay line for use with the inductive pickup. The third section presents measurements of phase shifter performance such as phase linearity, operation at low signal frequencies, effect of delay-line termination, signal amplitude distortion, effect of ambient-temperature variation, and operating range for two values of carrier frequency.

## CIRCUIT ANALYSIS

Figure 1 is a block diagram of the heterodyne phase shifter. Signal input to the phase shifter is fed to the input balanced mixer simultaneously with a fixed-frequency carrier with a controllable phase angle obtained via delay line 1. The resultant suppressed-carrier output is introduced into a single sideband filter which removes the lower sideband. The upper sideband is then retranslated

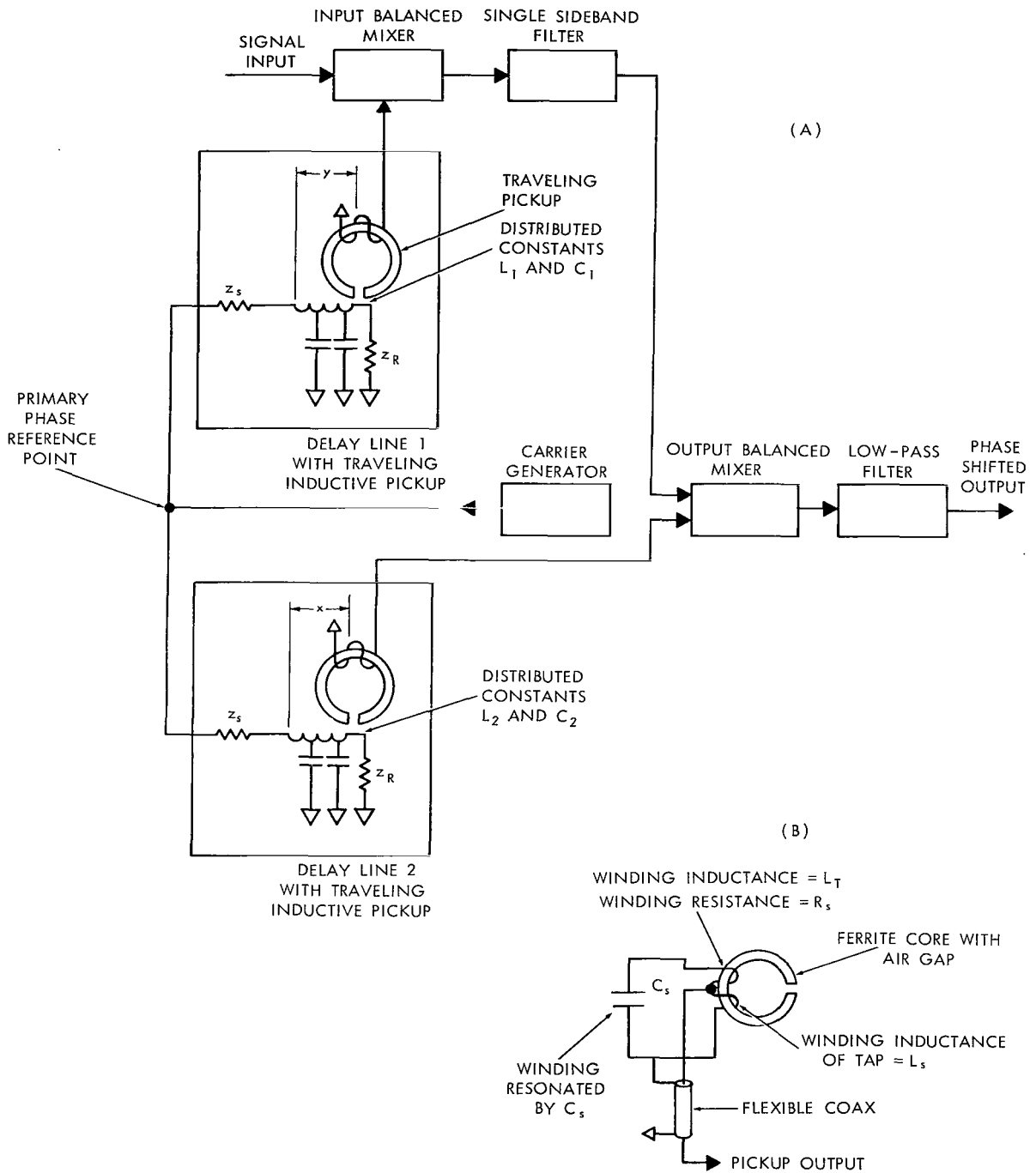


Figure 1—Block diagram of phase shifter (part A) with schematic diagram of traveling pickup with output taken from flexible coaxial cable (part B).

to signal frequency in the output balanced mixer. Carrier input to this modulator is phase-controlled by delay line 2. The signal output of the system is taken from a low-pass filter following the output balanced mixer. The analysis will show that the output phase shift at the signal frequency is the

difference of the phase shifts introduced by the individual delay lines. The use of two delay lines rather than one offers more convenient operation. Delay line 2 provides a calibrated phase shift over a 360-degree range which is independent of signal frequency. Delay line 1 compensates for the frequency-dependent phase shift which occurs in the single sideband filter. In operation, delay line 1 establishes the zero phase shift point of the output for any given signal frequency, and the desired phase shift is then dialed with delay line 2. The variable-phase output of either line is obtained inductively with a gapped toroidal pickup (Figure 1, part B) which is moved parallel to the delay-line axis. The line and pickup are considered in Appendix C. The analysis is limited to showing that the pickup output voltage is a replica of the delay-line current in the vicinity of the pickup. The derivation does not attempt to predict the pickup voltage in terms of the geometry of the system (e.g., relating the output voltage to the radial distance from the line). Since the analysis is quoted in the text without restating the basic underlying assumptions, they are summarized here:

- (1) The delay lines have distributed constants and are lossless.
- (2) The pickup and line are treated as a transformer with a mutual inductance coupling parameter.
- (3) The presence of the pickup does not alter the line current.

The order to be taken in making the analysis follows the order shown in the block diagram. There are two carrier paths fed from a common carrier generator; each path leads to the output balanced mixer, the output of which contains the phase-shifted signal. Since both paths originate in a common carrier generator, the output point of the generator is chosen as the primary phase reference axis. The signal input referred to this axis is assumed to have an initial zero phase angle, meaning that, if the carrier voltage is  $E_c \sin \omega_c t$  at this reference point, then the signal input is written as  $E_s \sin(\omega_s t + \omega_s t_0)$  with the initial condition that  $t_0 = 0$ . By setting  $t_0 = 0$ , the analysis is not restricted, since the relative phase between the output and input signals would remain unchanged if  $t_0 \neq 0$ ; however, the zero condition avoids carrying the term through the analysis. The analysis begins with the uppermost of the two carrier paths, the input balanced mixer and single sideband filter.

### **Input Balanced Mixer Equation**

A balanced mixer can be approximated as a product-forming device with respect to the useful frequencies appearing in the output (Reference 1). With a carrier input signal  $\sin \omega_c t$  and a signal input  $\sin \omega_s t$ , the principal frequency components in the output are  $\cos(\omega_c t - \omega_s t) - \cos(\omega_c t + \omega_s t)$ . The amplitude of these components can be made proportional to the input signal amplitude only under saturated conditions; i.e., if the carrier input is sufficiently large relative to the signal amplitude (see Figures 7 and 9). The amplitude of the output signal components, however, will be less than the amplitude of the input signal with the reduction depending on the type of circuit. For the type of circuit used as the input mixer in the experimental system, the amplitude of the output is of the order of 1/4 the signal amplitude under saturated carrier conditions. Saturated carrier conditions and an amplitude coefficient of 1/4 will be assumed for the input balanced mixer. According

to Appendix C, Equation C21, the output of the inductive pickup coupled to a correctly terminated delay line is of the form  $\sin(\omega_c t - z_0 \omega_c \sqrt{LC})$ , where

- $z_0$  = distance to center of the pickup gap from the line input,
- $L$  = distributed inductance per unit length, and
- $C$  = distributed capacitance per unit length.

Accordingly, in this case, the pickup output from line 1, which applies the carrier to the input mixer, can be written as  $\sin(\omega_0 t - y \omega_c \sqrt{L_1 C_1})$ , where

- $y$  = distance from the carrier input to line 1 to the center of the pickup gap,
- $L_1$  = distributed inductance, line 1, and
- $C_1$  = distributed capacitance, line 1.

For simplicity, the expression is written in the form  $\sin(\omega_c t - \theta_y)$  where  $\theta_y$  is the equivalent phase angle  $\theta_y = y \omega_c \sqrt{L_1 C_1}$ . With the carrier input previously given, and a signal input  $E_s \sin \omega_s t$ , the output of the first mixer can be written as

$$\frac{E_s}{4} \left[ \cos(\omega_c t - \theta_y - \omega_s t) - \cos(\omega_c t - \theta_y + \omega_s t) \right] \quad (1)$$

### Single Sideband Filter Equation

The transfer function of the single sideband filter is approximated with straight lines in Figure 2 (see Figure 8 for the plot of the characteristics of the crystal filter used in the experimental model). The upper curve in Figure 2 is a straight-line approximation of the output amplitude as the ordinate with the radian frequency as the abscissa, while the lower plot is an approximation of the output phase shift plotted against the same abscissa. Output phase and amplitude can be obtained for any input signal with frequency  $\omega$  by plotting  $\omega$  on the abscissa and then reading the amplitude coefficient on the upper curve; the phase is read from the lower curve. The input signal to the filter contains the frequency  $\omega_c + \omega_s$  and  $\omega_c - \omega_s$ , but not the carrier frequency  $\omega_c$ . However, to maintain phase continuity in the analysis, it is necessary to use the carrier frequency point on the abscissa and to determine the corresponding phase shift

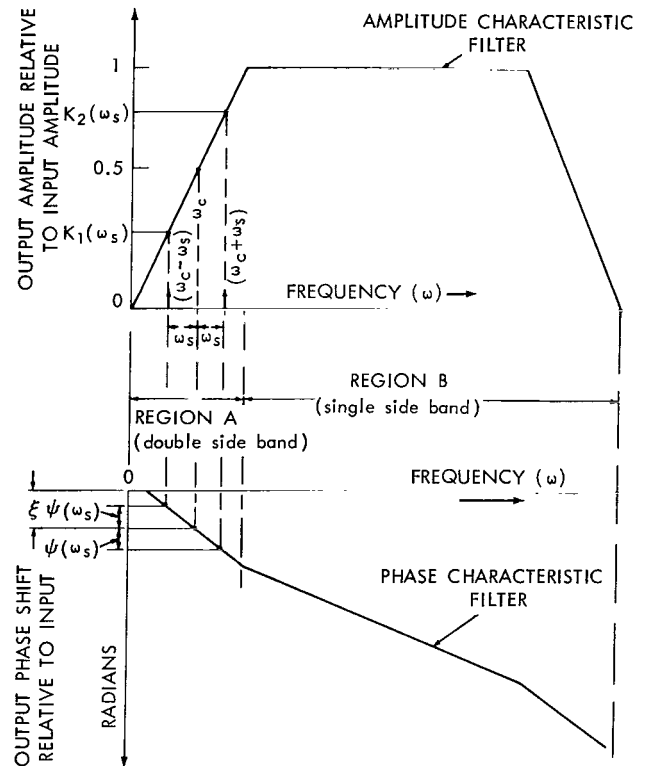


Figure 2—Filter amplitude-phase straight-line approximation showing placement of sidebands.

through the filter relative to this point. The phase shift angle corresponding to  $\omega_c$  is shown as  $\xi$  on the lower ordinate. The phase shift of the components  $\omega_c + \omega_s$  and  $\omega_c - \omega_s$  is measured relative to  $\xi$  as a variable angle  $\psi(\omega_s)$  on the lower ordinate, which is a function of the signal frequency  $\omega_s$  once  $\omega_c$  is fixed. Similarly, as shown on the uppermost ordinate, the amplitude coefficient  $K_1(\omega_s)$  corresponding to the lower sideband  $\omega_c - \omega_s$  and the amplitude coefficient  $K_2(\omega_s)$  corresponding to the upper sideband  $\omega_c + \omega_s$  are also functions of  $\omega_s$ . However, to save space, the functional relationship will not be indicated in future notation as is done in Figure 2. Accordingly, the output of the filter from an inspection of Figure 2 can be written as

$$\frac{E_s}{4} \left[ K_1 \cos(\omega_c t - \omega_s t - \xi + \psi - \theta_y) - K_2 \cos(\omega_c t + \omega_s t - \xi - \psi - \theta_y) \right] . \quad (2)$$

### Output Balanced Mixer Equation

Regeneration of the signal frequency takes place in the output balanced mixer; in addition, the output will contain the phase shifts introduced by both delay lines. The signal conversion factor under saturated carrier conditions will be assumed to be 1/3, the approximate factor measured for the output balanced mixer in the experimental circuit. The carrier input to the mixer can be written as  $\sin(\omega_c t - \theta_x)$ . Using Appendix C, Equation C21,  $\theta_x = x \omega_c \sqrt{L_2 C_2}$ , where

$x$  = distance from the carrier input line 2 to center of pickup gap,

$L_2$  = distributed inductance, and

$C_2$  = distributed capacitance, line 2.

The signal input to this mixer is derived from the single sideband filter and is given by Equation 2. The significant frequency components in the output of the mixer are obtained by taking the product of the carrier input and the signal input. This gives for the output

$$\frac{E_s}{12} \left[ K_1 \sin(\omega_s t + \xi - \psi + \theta_y - \theta_x) - K_2 \sin(-\omega_s t + \xi + \psi + \theta_y - \theta_x) \right] + \text{carrier-frequency terms} . \quad (3)$$

The unwanted carrier-frequency terms are removed in the low-pass filter following the mixer (Figure 1). The amplitude coefficient in the above equation is the product of the signal coefficient  $E_s/4$  from Equation 2 and the conversion factor for the mixer 1/3.

### Phase Shifter Output Expression, Normal Operation

According to Equation 3, the phase shifter output expression in the most general form is made up of the sum of two sinusoids at the signal frequency with amplitudes  $K_1$  and  $K_2$ . The negative sign preceding the signal frequency in the  $K_2$  term can be altered by use of the identity  $-\sin A = \sin(-A)$  to give

$$\frac{E_s}{12} \left[ K_1 \sin(\omega_s t + \xi - \psi + \theta_y - \theta_x) + K_2 \sin(\omega_s t - \xi - \psi - \theta_y + \theta_x) \right] . \quad (4)$$

Most significant to the operation of the phase shifter is the fact that the  $K_1$  component contains the phase angle  $\theta_y - \theta_x$ , while the  $K_2$  component contains the negative value of this angle,  $-\theta_y + \theta_x$ . Because of the reversal of sign, the components when represented as phasors will rotate in opposite directions if either  $\theta_x$  or  $\theta_y$  is varied. The sum of contrarotating phasors will exhibit both periodic phase and amplitude variation; the exact form of this variation is discussed further in the next section. Since it is desirable that the phase shifter output be constant with linear phase shift, it is necessary that the lower sideband be removed in the single sideband filter. This requirement places a lower limit on the frequency of the signal input to the phase shifter. Although the demarcation could not be expected to be so sharp in a practical device, the frequency axis of the idealized filter (Figure 2) has been divided into a double sideband region, region A, where  $K_1, K_2 \neq 0$  and a single sideband region, region B, where  $K_1 = 0$  and  $K_2 = 1$ . Normal operating range for the phase shifter is defined as the range of signal frequencies which permits the upper sideband to lie only in region B, the bandpass region of the filter. Throughout this range of signal frequencies,  $K_1 = 0$ ; thus the phase shifter output is the  $K_2$  term of Equation 4,

$$\frac{E_s}{12} K_2 \sin(\omega_s t - \xi - \psi - \theta_y + \theta_x) \quad (5)$$

To operate the phase shifter at any given signal frequency, the pickup distance  $y$ , line 1, is set to cancel the frequency-dependent phase shift in the single sideband filter. Because  $\xi$ ,  $\psi$ , and  $\theta_y$  are all lagging phase angles, the cancellation takes the form (with  $\xi$ ,  $\psi$ , and  $\theta$  expressed in degrees)

$$-\xi - \psi - \theta_y = n(-360), \quad \text{where } n \text{ is a positive integer.} \quad (6)$$

The term  $\theta_y$  need not have a range greater than 360 degrees to satisfy Equation 6. Although the filter phase shift  $-\xi - \psi$  may be several multiples of -360 degrees,  $\theta_y$  need only be of sufficient magnitude to bring the total angle on the left of Equation 6 to the nearest multiple of -360 degrees; for instance if  $-\xi - \psi = 739$  degrees,  $-739 - \theta_y = 3(-360) = -1080$ . Thus,  $\theta_y = 341$ ; if  $-\xi - \psi = 420$ ,  $-420 - \theta_y = 2(-360) = -720$ ; in this case,  $\theta_y = 300$ . Since zero degrees and integral multiples of -360 degrees are equivalent, the expression,  $-\xi - \psi - \theta_y$  is eliminated for Equation 5 to give for the phase shifter output

$$\frac{E_s}{12} K_2 \sin(\omega_s t + \theta_x) = \frac{E_s}{12} K_2 \sin(\omega_s t + x \omega_c \sqrt{L_2 C_2}) \quad (7)$$

The phase angle  $\theta_x$  introduced by line 2 is a linear function of pickup position  $x$ , with a slope dependent only on the oscillator frequency and the delay-line constants. Once the fixed errors are determined by calibration in a practical system, the calibration will be independent of signal frequency, since the same section of line will be utilized for a 360-degree phase-shift range. If line 1 were not provided for compensation, the zero point on line 2 would shift with signal frequency, and a different section of line would be required to span 360 degrees; thus a fixed calibration for error could not be used.

## Phase Nonlinearity and Amplitude Variation When Signal Frequency is Below Normal Operating Range

At signal frequencies below the normal operating range, the phase shifter output will contain both sideband terms as given by Equation 4 and will consequently exhibit undesirable phase and amplitude variation. The undesirable effect is essentially identical when either  $\theta_y$  or  $\theta_x$  is varied, and since  $\theta_y$  and  $\theta_x$  are not varied simultaneously, it is necessary only to consider the case for variation in  $\theta_x$ . Thus it will be assumed that delay line 1 is adjusted so that  $-\xi - \psi = \theta_y$ . With this adjustment,  $\theta_y$  is eliminated from Equation 4, and the phase shifter output is

$$\frac{E_s}{12} \left[ K_1 \sin(\omega_s t - 2\psi - \theta_x) + K_2 \sin(\omega_s t + \theta_x) \right] \quad (8)$$

This sum is combined into a single expression, Appendix B, Equation B7; the expression is repeated here.

$$\frac{E_s}{12} K_2 \left[ 1 + \frac{K_1^2}{K_2^2} + \frac{2K_1}{K_2} \cos(2\theta_x + 2\psi) \right]^{1/2} \sin \left[ \omega_s t + \theta_x - \tan^{-1} \frac{\frac{K_1}{K_2} \sin(2\theta_x + 2\psi)}{1 + \frac{K_1}{K_2} \cos(2\theta_x + 2\psi)} \right] \quad (9)$$

The resultant phase shifter output is characterized by amplitude and phase variations which are functions of  $2\theta_x$ ; the magnitude of both disturbances is determined by  $K_1/K_2$ , the ratio of the lower to upper sideband magnitude at the output of the single sideband filter.

An example of the phase and amplitude disturbance which results from the lower sideband is shown in Figure 3. Curve B is a plot of the cosine amplitude portion of Equation 9 versus  $\theta_x$  for the case  $K_1/K_2 = 0.2$ . Curve A is the same plot for the case  $K_1 = 0$ . Curve D is a plot of the phase-angle portion of Equation 9 versus  $\theta_x$  for the case  $K_1/K_2 = 0.2$ . Curve C is the same plot when  $K_1 = 0$ . All plots were made with  $E_s/12 = K_2 = 1$  and  $\psi = -30$  degrees.

The fact that the departure from phase linearity occurs simultaneously with output amplitude variation is a useful property in a practical system. Since both can be related to

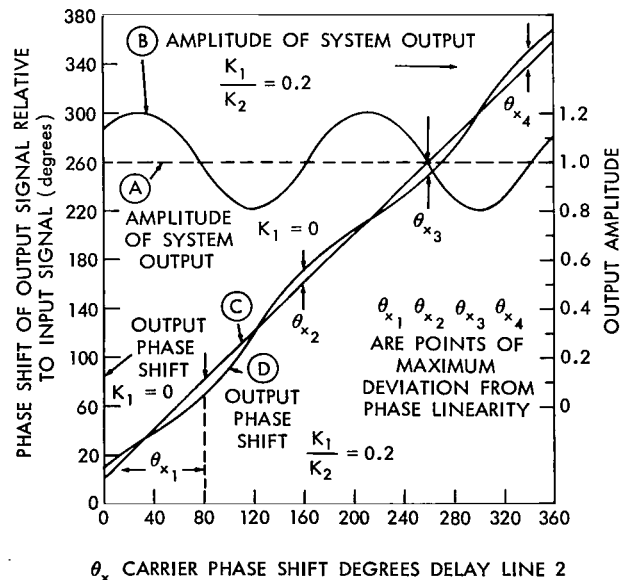


Figure 3—Phase and amplitude variation of system output caused by the lower sideband for the case  $K_1/K_2 = 0.2$ , and  $E_s/12 = K_2 = 1$ ,  $-\xi - \psi = \theta_y$ ,  $\psi = -30$  degrees.

$K_1/K_2$ , it is possible to determine the degree of phase nonlinearity at low signal frequencies from a simple measurement of output amplitude variation. (A later section will show that an improperly terminated delay line can also produce phase nonlinearity; however, this effect will not be dependent on signal frequency and in general will not be accompanied by amplitude fluctuation.) According to Equation B9, Appendix B, the sideband ratio  $K_1/K_2$  is related to the maximum and minimum value of the fluctuation in amplitude (observed while varying  $\theta_x$ ) by the equation

$$\frac{K_1}{K_2} = \frac{\max - \min}{\max + \min} (\text{output amplitude}) . \quad (10)$$

The value in degrees of the maximum phase departure from linearity (the maximum vertical distance between curves C and D at points  $\theta_{x_1}, \theta_{x_2}, \theta_{x_3}, \theta_{x_4}$  in Figure 3) corresponds to the maximum or minimum value of the arc tangent portion of the phase angle (Equation 9). The maximum or minimum value of this function in degrees, from Equation B8, Appendix B is

$$\pm \tan^{-1} \frac{\frac{K_1}{K_2}}{\left[1 - \left(\frac{K_1}{K_2}\right)^2\right]^{1/2}}, \quad \left(\frac{K_1}{K_2} < 1\right) . \quad (11)$$

Thus  $K_1/K_2$  can be determined from an amplitude measurement and substituted in the foregoing formula to determine the maximum departure from linearity. In the case of curve D with  $K_1/K_2 = 0.2$ , the maximum departure from linearity is  $\tan^{-1}(0.2/\sqrt{1-0.04}) = 11.5$  degrees.

According to Equation B10, Appendix B, the maximum value of the phase departure from linearity will occur when the amplitude of the system output has a value given by  $\sqrt{\max \min}$  (amplitude). Thus, in Figure 3, the maximum departure from linearity, curve D, will lie on a line with vertical intercepts passing through the amplitude plot at values of amplitude given by  $\sqrt{1.2} \times 0.8 = 0.98$ . The departure from linearity for the case  $K_1/K_2 = 0.2$  was shown to be 11.5 degrees. Several other values calculated with Equation 11 are

$$\frac{K_1}{K_2} = 10^{-3} (-60 \text{ db}), \quad \text{maximum departure from linearity} = 0.0573 \text{ degree};$$

$$\frac{K_1}{K_2} = 10^{-2} (-40 \text{ db}), \quad 0.573 \text{ degree};$$

and

$$\frac{K_1}{K_2} = 10^{-1} (-20 \text{ db}), \quad 5.73 \text{ degrees} .$$

The effects of the lower sideband place a lower limit on the frequency of the signal input, which in general will be determined by the attenuation rate of the front edge of the filter amplitude

characteristic, (region A). Selection of the oscillator frequency will also determine the minimum frequency of the signal input. Placement of the oscillator frequency in the center of region A appears to be the optimum choice for permitting the lowest possible minimum frequency. Such placement will permit maximum attenuation of the lower sideband and, at the same time, permit the upper sideband to have a reasonable amplitude. If region A is specified in kHz as extending from the frequency corresponding to maximum attenuation to the frequency corresponding to zero attenuation, then the minimum frequency will equal one-half the kHz value of region A. Minimum frequency so defined will permit the upper sideband to pass without attenuation while permitting maximum attenuation of the lower sideband. Maximum attenuation in a typical filter will be greater than -60 db; thus with the foregoing definition of minimum frequency,  $K_1/K_2 < 0.001$ , and the maximum departure from linearity will be less than 0.0573 degree.

While an oscillator frequency choice at the center of region A appears to be optimum in that it permits the lowest minimum signal frequency, it is not the only possible choice. For instance, if it is desired to phase-shift a higher band of signal frequencies, the oscillator frequency need only be chosen at a lower value and can, in fact, lie to the left of region A. It is required that the mixer bandwidth be sufficient to generate the upper sideband in the case of the input mixer, and regenerate the signal frequency in the case of the output mixer. The calibration of the delay lines will, of course, differ in this case because of the dependence of phase shift on carrier frequency.

### Phase Nonlinearity Resulting From Improperly Terminated Delay Lines

The preceding expression for phase shifter output, Equation 5, contains a phase angle  $\theta_x$  which is linear with respect to  $x$ , the distance measured from the center of the pickup gap to the carrier input point of line 2, since  $\theta_x = x \omega_c \sqrt{L_2 C_2}$ . Such a linear relationship is shown (Appendix C, Equation C22) to be possible only if the line is terminated in a load resistance equal to the characteristic impedance. If the line is not so terminated, the phase shifter output expression will contain an additional term which will cause deviations from linearity. It is particularly important that the phase shift provided by line 2 be linear since it is intended to provide a calibrated phase shift over an extended range. (Phase linearity of line 1 is of less importance; in the actual phase shifter circuit, the line is set with the aid of an auxiliary device so that line calibration is not required.) It will be assumed that the signal frequency is sufficiently high so that the single sideband filter removes the lower sideband ( $K_1 = 0$ ) and delay line 1 has been preset so as to compensate for the filter phase shift; i.e.  $\theta_y = -\xi - \psi$ . From Equation 2, the signal input to the output balanced mixer with the foregoing conditions is

$$\frac{E_s}{4} \left[ -K_2 \cos (\omega_c t + \omega_s t) \right] \quad . \quad (12)$$

The carrier input to the mixer when line 2 is improperly terminated will fluctuate in amplitude as  $\theta_x$  is varied. However, as previously indicated, the mixer output will be independent of carrier level if carrier level is above a minimum. It will be assumed that this is the case here. The general expression for the pickup output is given by Equation C19, Appendix C. This expression,

as applied to line 2 and written without the periodic amplitude factor, is

$$\sin \left( \omega_c t - \theta_x + \tan^{-1} \frac{R_r \sin \lambda}{1 + R_r \cos \lambda} \right), \quad (13)$$

where

$$\lambda = 2\beta x - 2\beta \ell + \phi + \pi,$$

$$\beta = \omega_c \sqrt{L_2 C_2},$$

$$\ell = \text{line length},$$

$$x = \text{distance from line input to center of pickup gap, and}$$

$$\beta x = \theta_x.$$

The significant parameter in the foregoing expression is the parameter  $R_r$ , the reflection factor. This factor is related to the characteristic impedance  $Z_0$  and the terminating impedance  $\bar{Z}_r$  by the expression

$$\frac{\bar{Z}_r - Z_0}{\bar{Z}_r + Z_0} = R_r e^{j\phi}. \quad (14)$$

The significant frequency components in the output of the second mixer are given by the product of the carrier input (Equation 13) and the signal input (Equation 12). With a 1/3 conversion factor for the mixer, this product is

$$\frac{E_s}{12} K_2 \sin \left( \omega_s t + \beta x - \tan^{-1} \frac{R_r \sin \lambda}{1 + R_r \cos \lambda} \right) + \text{carrier frequency terms removed in the low-pass filter following the mixer.} \quad (15)$$

A comparison of the phase shifter output given by Equation 15 with Equation 9 shows that an improperly terminated delay line causes a deviation from linearity which is similar to that produced by the lower sideband (with the exception of the constant phase angles present in the arguments of the sine and cosine terms). Particularly,  $K_1/K_2$  is exactly analogous to  $R_r$  as the significant parameter in the arc tangent terms. It will be recalled that the arc tangent term in Equation 7 resulted because of the summing of contrarotating phasors. In the case of reflection on the delay line, an analogous situation prevails. According to Equation C18, Appendix C, the pickup output from delay line 2 can be expressed as a sum by eliminating the negative sign preceding the  $R_r$  term with the expression  $-1 \equiv e^{j\pi}$ ; the contrarotating phasors are  $e^{-j\beta x}$  and  $R_r e^{j(\beta x - 2\beta \ell + \phi + \pi)}$ .

The maximum or minimum value of the arc tangent term resulting from improper termination, using the expression developed in Appendix D is

$$\tan^{-1} \frac{R_r}{\sqrt{1 - R_r^2}}. \quad (16)$$

Although in general the amplitude variation which accompanies the phase perturbation will not appear at the phase shifter output, measurement of the pickup output when the pickup traverses the line is a useful technique for evaluating the departure from phase linearity. Knowing the maximum and minimum, values of the amplitude variation  $R_r$  can be calculated from Equation C22:

$$R_r = \frac{ep(\max) - ep(\min)}{ep(\max) + ep(\min)}, \quad (17)$$

where  $ep$  = pickup output.

### Phase Shifter Output for Nonsinusoidal Input

If the input to the phase shifter is other than a sine wave, the output will be distorted. This distortion is a consequence of the fact that the controllable phase-shift angle  $\theta_x$  is independent of the signal frequency  $\omega_s$ . To reproduce a complex wave at the output with controllable delay, it is necessary that the relative amplitudes of the individual components be preserved and each component be delayed by an equal amount of time; this latter requirement cannot be met by the phase shifter. If the input be represented by  $e_1 \sin \omega_s t + e_2 \sin 2 \omega_s t + e_3 \sin 3 \omega_s t \dots$ , then a nondistorted output will be of the form  $e_1 \sin \omega_s (t - t_d) + e_2 \sin 2 \omega_s (t - t_d) + e_3 \sin 3 \omega_s (t - t_d)$ . The phase angle of each output component is seen to be  $-\omega_s t_d, -2 \omega_s t_d, -3 \omega_s t_d$ ; i.e., the phase angle magnitude increases linearly with respect to the signal frequency  $\omega_s$ . The phase shifter output for a single frequency is given by Equation 5 as  $E_s/12K_2 \sin(\omega_s t - \xi - \psi - \theta_y + \theta_x)$ . It will be recalled that the angle  $\psi$  is a function of  $\omega_s$ , and in an ideal filter would vary linearly with  $\omega_s$ . In this case, assume that  $\psi = -P \omega_s$ . To further simplify the discussion, let delay line 1 be adjusted so that  $-\xi - \theta_y = 0$ , and normalize the amplitude coefficient  $E_s/12K_2 = 1$ . The output for a single frequency under these conditions is  $\sin[\omega_s (t - P) + \theta_x]$ . If the input to the phase shifter is a complex waveform,  $e_1 \sin \omega_s t + e_2 \sin 2 \omega_s t \dots$ , the output will be  $e_1 \sin[\omega_s (t - P) + \theta_x] + e_2 \sin[2 \omega_s (t - P) + \theta_x] + e_3 \sin[3 \omega_s (t - P) + \theta_x] \dots$ . From an inspection of this expression, it is evident that even though the filter phase angle  $\psi$  be linear with signal frequency, the resultant output does not contain a total phase angle which varies linearly with signal frequency, because of the addition of the constant phase angle term  $\theta_x$  to each component; thus, the output will be distorted.

## PHASE SHIFTER DESIGN AND CONSTRUCTION

### Block Diagram

Figure 4 shows the phase shifter block diagram, which is identical with the theoretical system with respect to major blocks but employs the following additional circuits: (1) two carrier amplifiers supplying the balanced mixers, (2) a single sideband amplifier mounted on a common chassis with the crystal filters, (3) a variable gain-signal amplifier as the output stage, and (4) four emitter followers for impedance transformation or isolation. Additional information pertaining to the

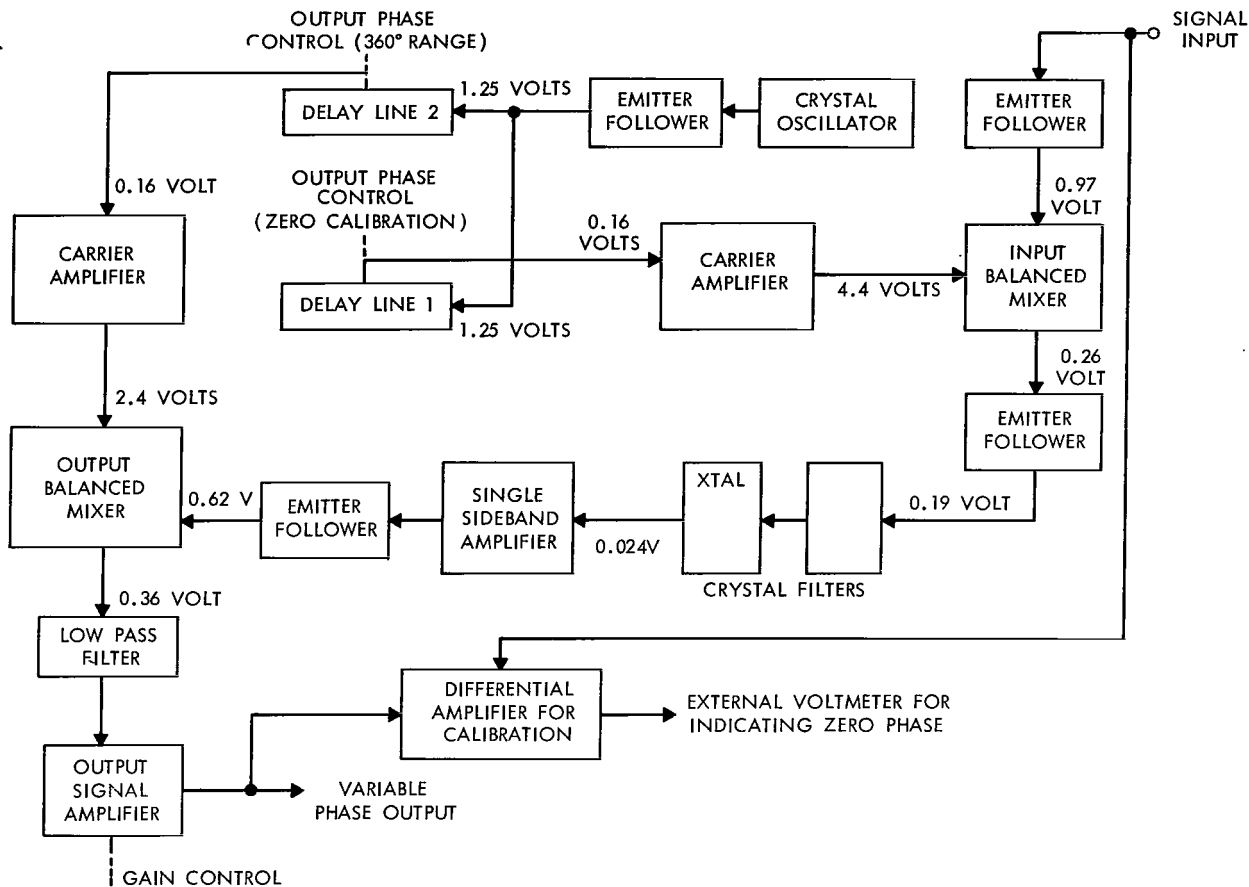


Figure 4—Block diagram of experimental heterodyne phase shifter showing input-output frequency and rms voltage for each block (input = 50 kHz, 1 volt rms).

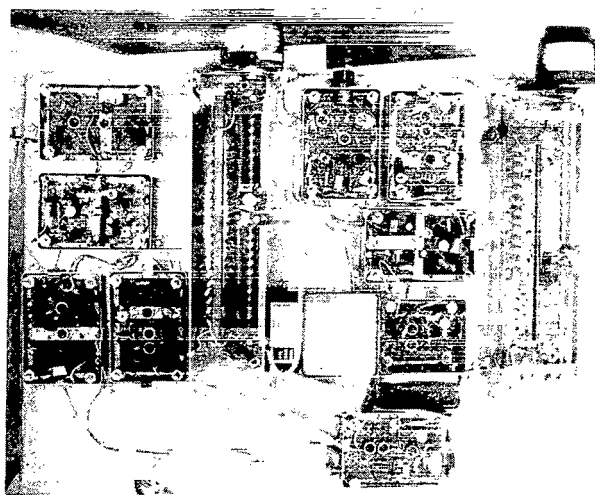


Figure 5—Phase shifter layout.

system layout can be obtained by examination of Figure 5. Each module, with the exception of the crystal filters and single sideband amplifier, is fabricated on a circuit board sized to fit in a 2-1/4 x 3-1/4 x 7/8-inch brass case. Four screws mounted in the corners of the case secure the circuit board to the case. A second identical case provides the cover which is drilled to permit the screw to extend through holes in the corners. The cases are secured to a copper-covered plywood base by external lugs held by the corner chassis screws. This method offers quick fabrication and easy disassembly and provides shielding (not particularly critical because of the relatively large voltage levels). However,

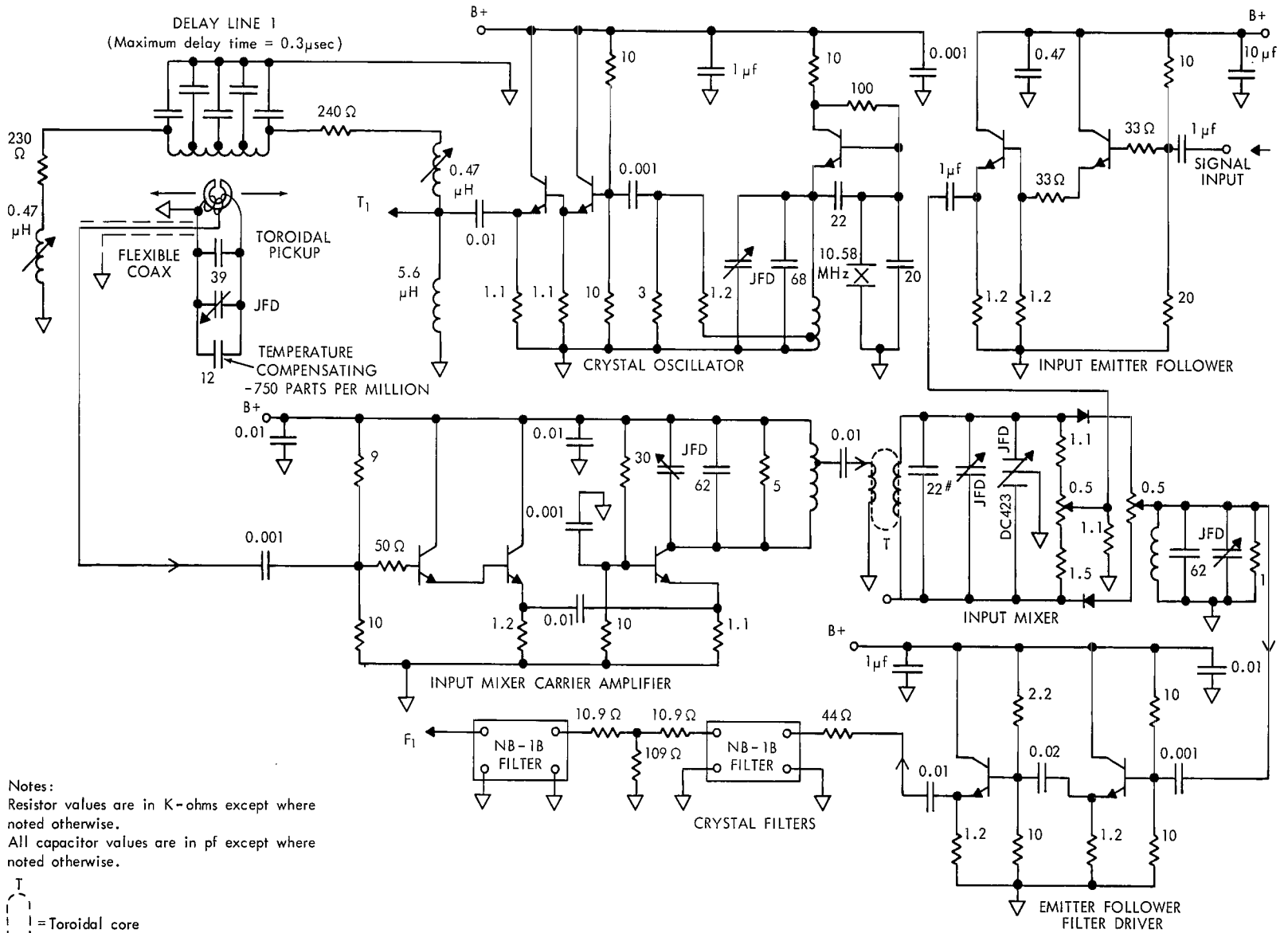
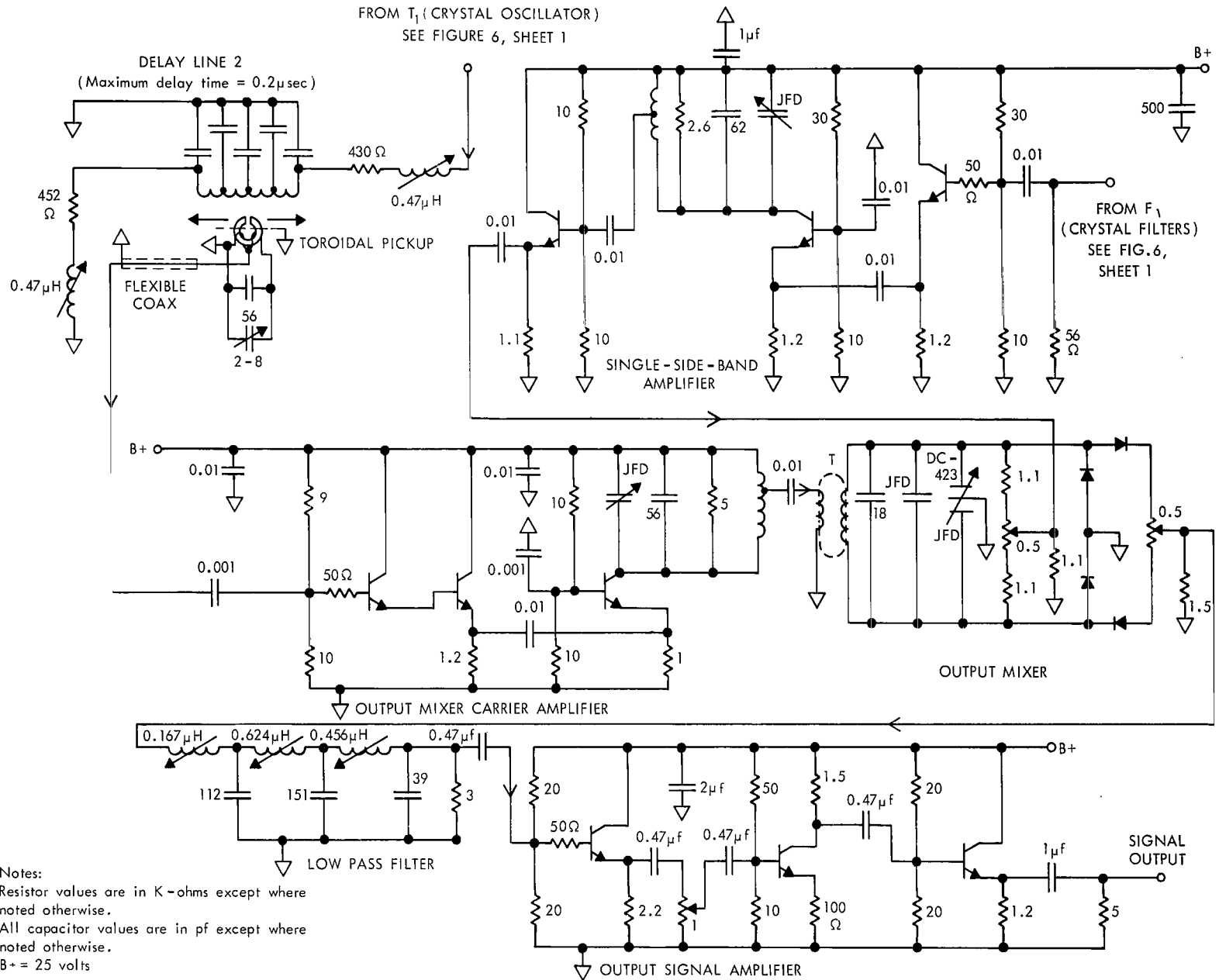


Figure 6—Phase shifter schematic diagram (sheet 1).



Notes:  
Resistor values are in K-ohms except where noted otherwise.  
All capacitor values are in pf except where noted otherwise.  
B+ = 25 volts

Figure 6—Phase shifter schematic diagram (sheet 2).

the crystal filters do require careful shielding; these were mounted in slightly larger cases to form an integral unit with the single sideband amplifier.

A more detailed description of the individual circuits comprising each module follows. The complete circuit diagram is shown in Figure 6, sheets 1 and 2 with pertinent detail concerning components in Table 1.

Table 1

Component Data.

- (1) All transistors 2N2217
- (2) All resistors 1/4 watt except where noted
- (3) Total current input to phase shifter = 148 ma at +25 volts

Circuit	Remarks
Signal input emitter follower	Current: Input transistor 13 ma, output transistor 10 ma (heat sink) Input impedance: 6 kohms
Input balanced mixer	Diodes: Clevite fast-switching silicon mesa, CMD 7103 Capacitors: Trimmer, JFD MC 623, 28 $\mu\mu$ max., Differential, JFD DC 423 Core: Carrier input transformer, Gen. Ceramics F 624-2-Q-2, primary 6 turns insulated #27, secondary 12 turns #27 Output coil: 28 turns, #29 enamel, 0.25-inch, ceramic dia. form Potentiometers for balancing: Bourns RT 22 Resistors T-network: Weston Precision Metal Film 1/8 watt
Emitter follower driver for crystal filter	Current: Input transistor 12.5 ma, output transistor 14.5 ma (heat sink), 1/2-watt emitter resistor
Crystal filters	Midland, NB-1B, 10.7 MHz
Single sideband amplifier	Current: Input transistor 5 ma, voltage amplifier stage 5 ma, emitter-follower output 11 ma Coil: 28 turns, #29 enamel, 0.25-inch dia. ceramic form, tap 10 turns from B+ end Capacitor trimmer: JFD MC 623
Output mixer	Essentially similar to input mixer with the exception of additional diodes
Input balanced mixer carrier amplifier	Current: Input transistor 6 ma, output transistor 13 ma, heat sink Coil: 28T, #29 enamel, 0.25-inch dia. ceramic form, tap-10 turns from B+ end Capacitor trimmer: JFD MC 623
Output balanced mixer carrier amplifier	Current: Input transistor 0.5 ma, emitter follower 11 ma (These two transistors constitute direct-coupled Darlington) Output stage 11 ma, heat sink Coil: 28 turns, #29 enamel, 0.25-inch dia. ceramic form, tap-10 turns from B+ end Capacitor trimmer: JFD MC 623
Oscillator	Crystal, midland, CR-33, 10.580 MHz, parallel resonant Coil: 28 turns, #29 enamel, 0.25-inch dia. ceramic coil form, tap-10 turns from ground end Capacitor: JFD MC 623 Current: Oscillator stage 1 ma, Darlington output 19 ma

Table 1 (Continued)

Circuit	Remarks
Low pass filter	Adjustable inductors: Essex VIV, 470, 680, and 220 $\mu$ H
Output signal amplifier	Current: Input emitter follower, 4.5 ma, Voltage amplifier, 7 ma, Output emitter follower 12 ma Minimum load at 1-volt output, for no distortion = 300 ohms
Delay line 1	Ad-Yu. 0.3 $\mu$ sec., 200-ohm, type 557SN1; modified mechanically (see text); all capacitors replaced with 1% values; pickup coil, 10 turns #32 enamel wire, tapped 4th turn from ground end; core: Gen. Ceramics F 625-2-Q2 with 0.013-inch radial gap; trimmer capacitor: JFD VC 9G
Delay line 2	Ad-Yu. 551S, 0.22 $\mu$ sec, 400-ohm; modified mechanically (see text); all capacitors replaced with 1% values; pickup coil, 10 turns #32 enamel wire, tapped 4th turn from ground end; core: Gen. Ceramics F 625-2-Q2 with 0.013-inch radial gap; trimmer capacitor: JFD VC 9G

### Input Balanced Mixer

The input balanced mixer generates an upper and lower sideband displaced from the carrier by a frequency differential equal to the signal frequency. The lower sideband is then eliminated by a bandpass crystal filter; the upper sideband is used to regenerate the signal frequency by heterodyning with the carrier again in the output mixer. A balanced-type mixer was selected at the input to eliminate the carrier which would otherwise pass through the filter (somewhat attenuated) to the output mixer where it would cause an undesired phase shift of the regenerated signal appearing at the phase shifter output. The input balanced mixer circuit is a half-wave, carrier-controlled diode switch which transfers the signal to the output on positive excursions of the carrier. Switching takes place in two series diodes driven to conduction by a voltage supplied by a tuned-secondary, carrier-input transformer. An adjustable electrical center tap to ground for the secondary is established by a potentiometer and a 1.1 kohm resistor in a T network. The signal is brought in at the shunt arm of the T. When the diodes are conducting, the signal is switched to the load in parallel paths consisting of the series arms of the T network and the diode forward resistance. The carrier does not appear in the output because the T network and series diodes form a balanced-bridge configuration. Balancing for carrier elimination is accomplished by adjustment of the potentiometer in the center of the T network in conjunction with adjustment of the differential transformer placed across the carrier transformer secondary. Fine adjustment is provided by a second potentiometer with the center arm connected to the mixer output terminal; this potentiometer compensates for differences in the diode forward resistances.

The output load for the mixer is a tank circuit tuned to 10.7 MHz; the tank is paralleled with a 1-kohm resistor to permit a wide bandwidth. Efficient generation of sidebands occurs with signal

frequencies well beyond 500 kHz. The tank circuit shunts the large unwanted component at signal frequency (this component is characteristic of half-wave carrier switching). Input carrier level to the mixer is an important consideration: The data plotted in Figure 7 show that the useful output, the first sideband pair, becomes independent of carrier level if the level is above 1 volt, while minimum distortion requires the level to be above 2 volts. Normal operating carrier level was chosen to be 3.1 volts.

### Input Mixer Carrier Amplifier

A grounded-base, power-amplifier stage driven by a Darlington input stage drives the first mixer carrier transformer primary. A tap on the power-stage collector tank coil ensures optimum power match with the primary. The Darlington input circuit presents a 6-kohm load to the delay line pickup which drives the amplifier. Power matching is not employed in this case since it is desirable to avoid loading the pickup.

### Signal Emitter Follower

A Darlington circuit supplies the signal to the center of the first mixer T network. This stage is necessary because of the low impedance at this point, and in addition, helps prevent carrier feedback to the signal input terminals. The 33-ohm resistors in the base circuits prevent high-frequency oscillation which would normally occur if a coaxial cable were used to conduct the signal to the input terminals (these resistors are not needed in any of the other Darlington circuits).

### Crystal Filter

The crystal filter is the most critical component in the phase shifter circuit. An ideal filter for this application should have the following characteristics: (1) Infinite attenuation at the lower passband edge in a zero differential frequency interval, (the upper passband attenuation rate is of secondary importance); this characteristic would permit the lower sideband to be attenuated in a zero-frequency increment, thus permitting extension of the operation frequency range of the phase shifter to zero input frequency. (2) Infinite bandwidth in the bandpass region; the operating frequency range of the phase shifter could be made very high; its limit would then be determined by the carrier frequency, the bandwidth of the mixer circuits, and the bandwidth of the amplifier in the upper sideband signal path. (3) Constant phase shift independent of frequency in the bandpass region; the phase shifter zero-phase calibration-point variation with input frequency would then be determined by mixer phase characteristics and the amplifier used in the upper sideband signal

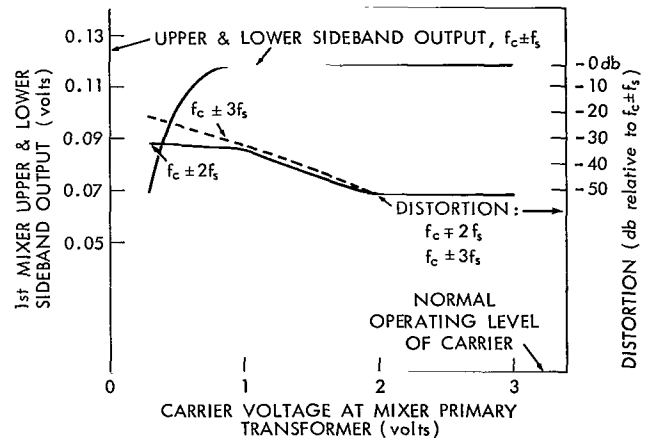


Figure 7—Input mixer output versus carrier input ( $f_s$  = signal frequency, 50 khz at 0.5 volt,  $f_c$  = carrier frequency).

path. The variation in calibration point with input frequency could then be made small enough to eliminate the need for two delay lines. The first requirement is most nearly met by the use of commercial single sideband filters which exhibit lower cutoff attenuation rates as great as 58 db in 600 Hz; however the bandwidth is limited to 6 kHz or less. The requirement of constant phase shift cannot be met by any standard filter available without the use of all-pass networks, a difficult design where a large bandpass region is required.

The filter selected, a Midland-type NB-1B, is a compromise favoring bandwidth at the expense of cutoff rate. The filter incorporates four crystals to give a symmetrical wideband Chebyshev response. In order to increase the cutoff rate, two filters were cascaded; the necessary isolation between filters was provided with a 50-ohm T-pad. Measured phase and amplitude characteristics of the cascaded filters are shown in Figure 8. These data show the overall bandwidth at the 1-db points to be 180 kHz. Region A (see Figure 2) is approximately 60 kHz with a maximum measured attenuation of at least 60 db. The measured phase slope is  $-5.76$  degrees per kHz;

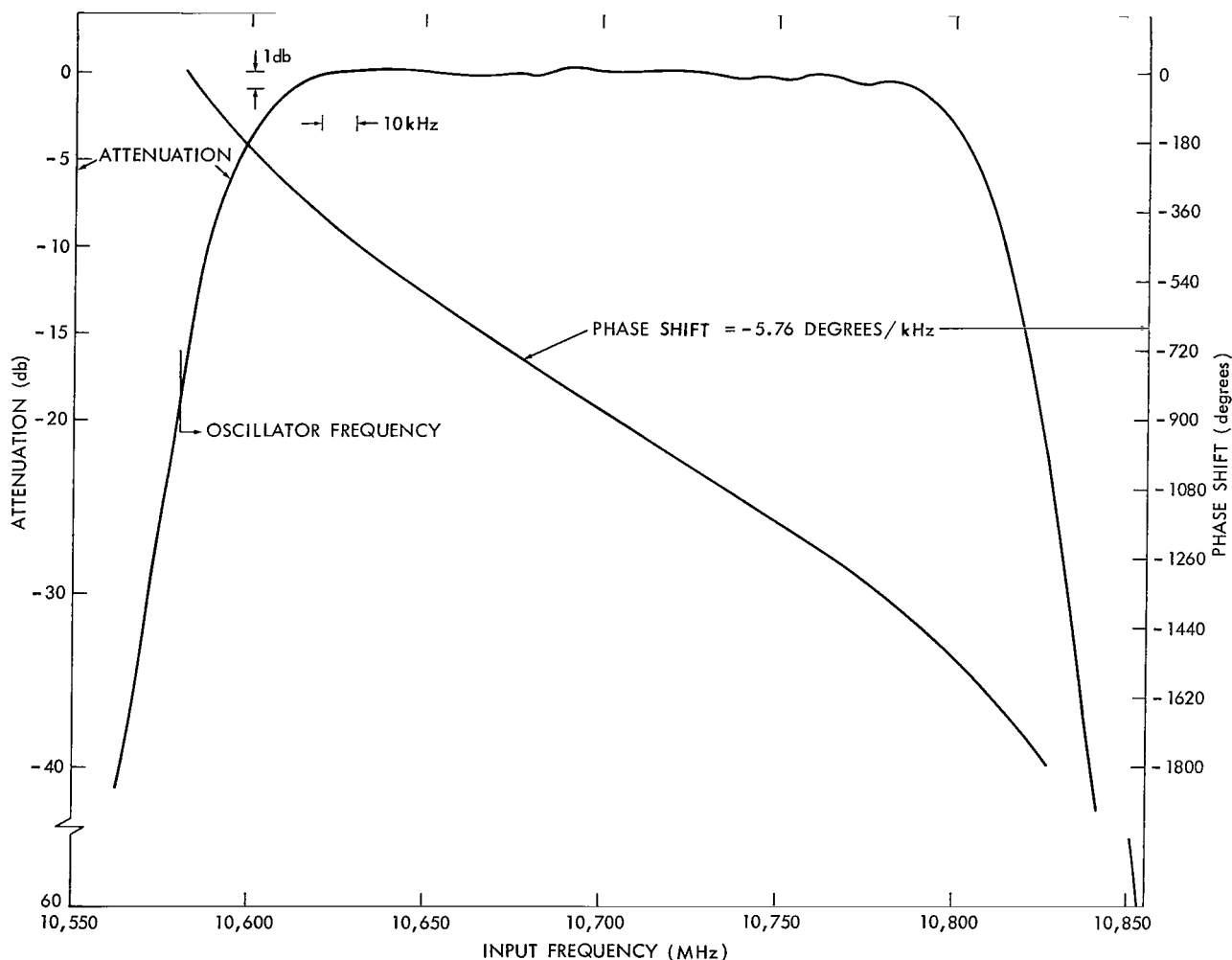


Figure 8—Phase and attenuation characteristics of tandem NB-1 crystal filters.

consequently the compensation (Equation 6) required of delay line 1 is 5.76 degrees for each 1-kHz increment in signal frequency.

### Emitter Follower Filter Driver

The 50-ohm input impedance of the crystal filter requires a low source impedance; consequently a Darlington emitter follower was used as the driver. The 3-ohm output impedance of the circuit was increased to 50 ohms by means of a 47-ohm series resistor. This circuit proved to be rather critical in respect to distortion; 15 ma of current was required in the output stage with the consequence that a heat sink for the output transistor is a definite requirement.

### Single Sideband Amplifier

To compensate for insertion loss, the filter is followed by a single sideband amplifier. The amplifier utilizes a grounded-base output stage driven by an emitter follower. The bandwidth requirements for the output stage are met by shunting the tank with a 2.6-kohm resistor. An emitter follower output stage is used for isolation. Without this stage for isolation, carrier leakage back from the second mixer causes intermodulation in the tank circuit.

### Output Mixer

Regeneration of the signal frequency takes place in the output mixer. The circuit is a half-wave carrier switch identical with the input mixer except for the addition of a second pair of diodes which shunt the carrier transformer secondary. This pair are provided with a center path to ground and are polarized to conduct when the diodes supplying the mixer output circuit are biased off by the carrier. The additional diodes improve efficiency at low output frequencies. Figure 9 shows

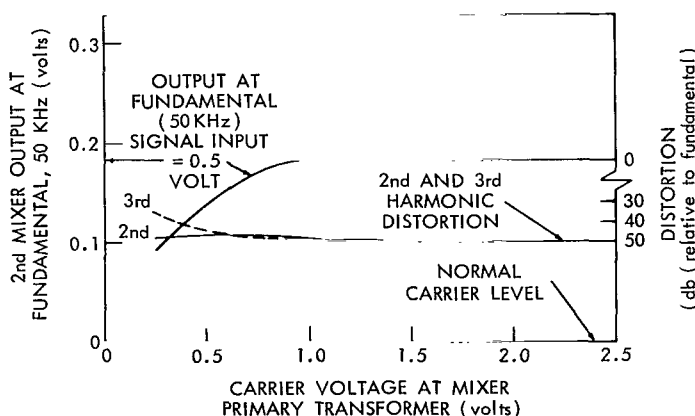


Figure 9—Output mixer output vs carrier voltage (upper side-band input = 0.5 volt, frequency = carrier frequency 50 kHz).

the output signal level and distortion versus the input carrier level. The output signal level becomes independent of the carrier level when the carrier level is 1 volt (signal level = 0.5 volt). Normal operating carrier level is maintained at 2.4 volts. The distortion characteristics are somewhat flatter relative to the carrier level when compared with the input mixer.

### Output Mixer Carrier Amplifier

The carrier input for the output mixer is taken from an amplifier which is similar to the carrier amplifier supplying the input mixer.

## Low-Pass Filter and Output Signal Amplifier

Although the carrier does not appear in the output of the last mixer (with proper adjustment of the differential capacitor and potentiometers), there is a component at the upper sideband frequency. This component is attenuated 60 db by the 6-pole Butterworth filter which follows the mixer. The filter design (Reference 2) places the corner frequency at 1 MHz and permits a flat response to 500 kHz.

The low-pass filter drives the output signal amplifier, which provides sufficient gain to bring the phase shifter output to 1 volt. A variable gain control is provided to compensate for variation in output level with input frequency (resulting primarily from ripple in the crystal-filter passband). This circuit consists of an emitter follower input to avoid loading the low-pass filter, one stage of voltage gain, and an output emitter follower to assure low-impedance source for the phase shifter output terminals.

## Crystal Oscillator

The carrier source for the phase detector is taken from a crystal oscillator, (Figure 6). This circuit consists of a crystal oscillator driving a Darlington emitter follower to provide a low-impedance source for driving the delay lines. The crystal, located in the base circuit of the oscillator stage, operates in the parallel resonant mode. The output from the oscillator is taken from a tank circuit in the emitter. The crystal filter (10.58 MHz) was selected to place the carrier frequency approximately in the center of the lower bandpass edge of the crystal filter attenuation plot, Figure 8.

## Delay Line 2

Delay Line 2 introduces a calibrated, 0- to 360-degree phase shift to the second mixer carrier input; this phase shift is transferred to the phase shifter output terminals by the heterodyne process. Accuracy of calibration requires that the phase shift introduced by the line be linear with respect to the line pickup position. The line is a standard commercial unit, Ad-Yu model 551-S, which was converted for use with the inductive pickup. The electrical characteristics as specified by the manufacturer are characteristic impedance = 400 ohms, bandwidth at the 3-db points = 25 MHz. The line, selected to have maximum delay time of 0.22 microsecond, is a lumped-constant type made with a continuous solenoid wound on a fiber rod and tapped at uniform intervals for junction with shunt capacitors. To improve linearity, these latter were replaced with 1-percent values.

The line as received from the manufacturer utilized a sliding contact to provide variable delay. The difficulties associated with the contact when used in the phase shifter circuit were: (1) The resolution was limited to 1.5 degrees, (2) The output from the contact showed small perturbations in phase and amplitude, which probably resulted because the contact shorted a turn as it moved along the line, and (3) The contact was occasionally found open-circuited, a difficulty which required cleaning the solenoid wire surface. The inductive pickup method was found to eliminate these difficulties, particularly since its use provided continuously adjustable phase shift which was not limited by the line solenoid winding density.

Figures 10 and 11 show how to install the inductive pickup without a major alteration of the mechanical structure of the line. The pickup positioning mechanism is a lead screw driving a threaded teflon carriage block parallel to the line solenoid. The lead screw is connected to a Borg Microdial 10-turn indexing head. A 4-digit head is preferable (a 3-digit head was used on the phase shifter prototype). The line is an integral self-supporting structure made up of inner and outer fiber rods and a copper ground strap, all fitted into fiber end blocks. The line is wound on

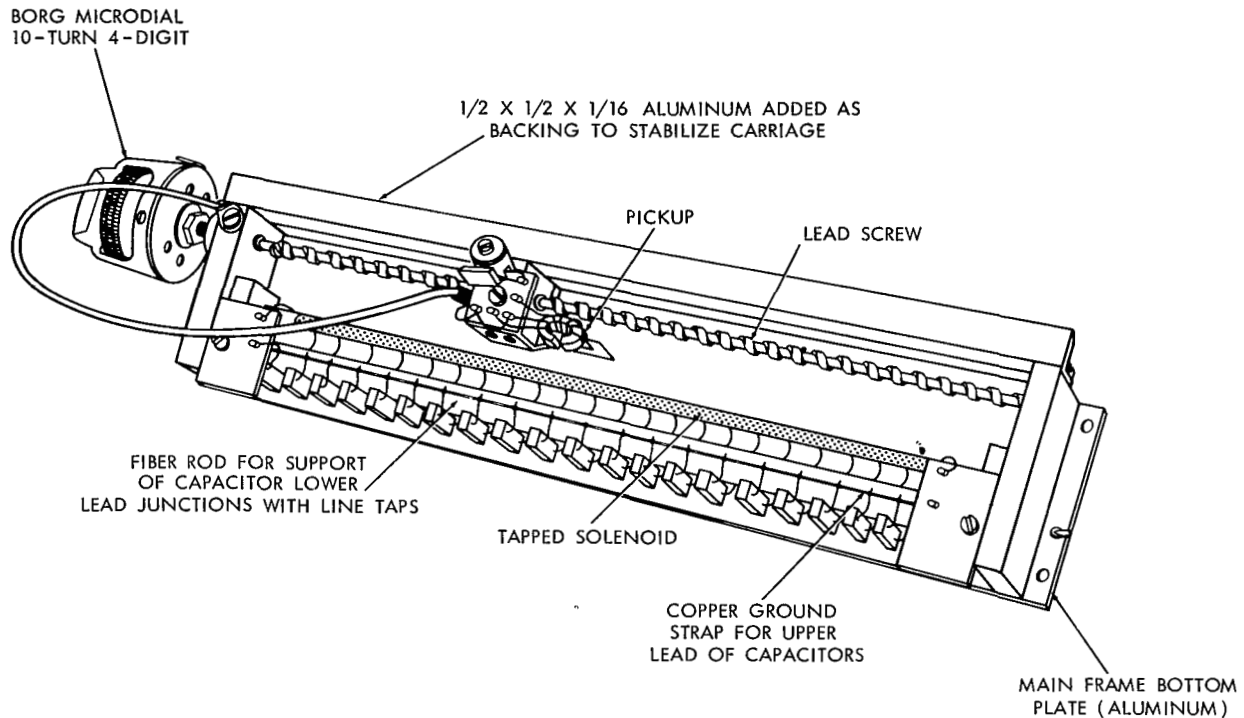


Figure 10—Modification of the AD-YU 557SN1 delay line for electromagnetic pickup, line 2.

the inner rod, while the outer rod supports the capacitor lower-lead junctions with the line taps. The copper ground strap provides a ground junction for the upper leads of the line capacitor. Conversion of the line calls for removal of the contacts and mounting of the pickup on the carriage block, increasing the spacing between the block and line and, finally, providing additional bearing surface for stabilizing the carriage. The spacing modification is made first by moving back the integral structure comprising the line and capacitors to permit 1/4-inch space between the line and the front of the

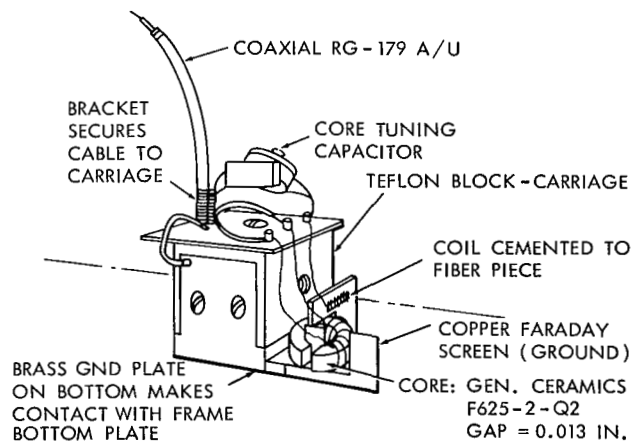


Figure 11—Pickup mounting details.

carriage block surface. The fiber end blocks of this structure are anchored with screws through the bottom frame plate (Figure 10). A 1/2 x 1/2 x 1/16-inch aluminum angle is then added to butt against the vertical surface of the carriage block; this added surface prevents skewing of the teflon block during pickup positioning. The method for mounting the pickup on the Teflon carriage block is shown in Figure 11. The sliding contact installed by the manufacturer is removed from the carriage, and an insulated terminal plate secured to the top of the carriage to provide for a tuning capacitor and coil lead termination. The flexible coaxial cable, which provides output from the pickup coil, is then secured to the side of the carriage with a bracket. Capacitance between the cable surface and tuning capacitor must be minimized; otherwise flexing of the cable during carriage motion will detune the pickup coil and adversely effect linearity. The toroid comprising the core of the pickup winding (General Ceramics F 625-2-Q2) is sliced radially for a 0.013-inch air gap and then wound according to Table 1. The completed coil is then cemented with epoxy to a slotted fiber piece.

The coil assembly is mounted on the side of the teflon carriage with a screw through the slot in the fiber piece; the slot provides a method for adjustment of the distance between the pickup and the line. To shield the coil winding and prevent capacitive coupling to the line, a grounded copper plate is installed to form a Faraday screen. The plate is in the form of an inverted E with the center leg projecting through the toroid. The E shape avoids forming a shorter turn.

Figure 12 shows the pickup electrical circuit. Ground for the coil, Faraday screen, and the outer braid of the coax is provided by a sliding plate mounted on the bottom of the teflon carriage; this plate contacts the main frame bottom plate. The grounded coil lead should be positioned nearest the winding surface of the delay line.

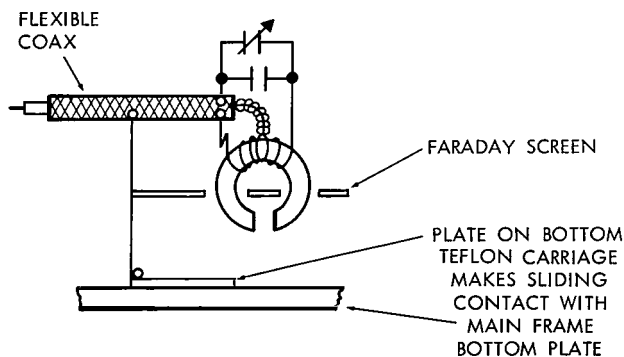


Figure 12—Pickup circuit.

The pickup gap provides electromagnetic coupling to the delay line (further details are given in Appendix C). Adjustment of the distance between the gap and the line as provided by the slotted fiber mount is an important consideration. The lumped-constant line solenoid showed a small electrical discontinuity at each capacitor tap. The discontinuity is evident as a perturbation in output voltage observed with both the ohmic contact and inductive pickup. However, with the pickup, the perturbation can be minimized by increasing the pickup spacing. A spacing of 0.172 inch (1.7 times the line radius) was found to be a

good choice of spacing. The output voltage from the pickup will decrease as the spacing increases. However, the falloff is not rapid; the output is 0.42 volt with the pickup at the line surface and 0.17 volt with 0.172-inch spacing.

The 0.22-microsecond time delay provides a carrier phase shift of almost twice 360 degrees at 10.580 MHz. This excess line length was chosen to permit the use of a lower carrier frequency

value when it is desired to shift the operating frequency range of the phase shifter upwards. Furthermore, it is necessary to select a line electrically longer than is required to phase-shift the carrier 360 degrees because pickup travel must be limited so that the pickup does not travel closer than approximately 1/2 inch from either end of the line winding (total winding length = 6 inches). Beyond these limits, the pickup output falls off — a consequence of the fact that the pickup couples to a finite section of line, rather than a single point on the line as in the case of the sliding contact.

## Delay Line 1

Delay Line 1 provides for adjustment of the phase of the first mixer carrier in order to cancel the phase shift introduced by the crystal filter. The line is not required to be calibrated accurately since the adjustment is guided by the null indication on the differential amplifier voltmeter. The line is an Ad-Yu, Model 557SN1,  $Z_0 = 200$  ohms. Total delay is 0.3 microsecond, which produces a maximum carrier phase shift of approximately 1100 degrees. The choice of a line 1100 degrees long is arbitrary since only 360 degrees are required for filter correction (Equation 6). However, the longer line offers more convenient operation. Conversion of the line for use with the inductive pickup is quite similar to the method shown previously with one minor mechanical difference — the integral structure supporting the line and capacitors is made from a single piece of slotted fiber (the structure can be removed from the main frame of the delay line as in the previous line). The line solenoid is mounted in the center of the slot which runs lengthwise. The slot is paralleled with copper strips which are part of the pickup contact mechanism. These strips are considered undesirable for pickup use since they are likely to affect the coupling process. However, since the line is not as critical with respect to linearity, the strips were not removed. To increase the spacing for pickup use, the line structure was raised in the supporting slots of the main frame. The pickup coil, tuning capacitor, and cable were mounted on the top surface of the teflon carriage block (the lead screw and block are similar to the previous line). A Borg microdial was again used for indexing. The coil and circuit are identical with that previously shown, except that the Faraday screen is not used. Spacing between the toroid gap and line is about 0.172 inch. Here again this adjustment is less critical than in the case of line 2.

## Differential Amplifier Circuit

Figure 13 shows the differential amplifier provided for indicating phase coincidence between the phase shifter input-output signal. This circuit functions as a calibrator which enables adjustment of delay line 1 to compensate for the phase shift in the crystal filter. Phase coincidence is indicated by a voltage null read on an auxiliary voltmeter driven by the differential amplifier. The circuit utilizes field effect transistors. Transistor  $Q_1$  functions as a differential amplifier, and  $Q_2$  and  $Q_3$  are source followers. A differential voltage appears at the load resistor in the drain of  $Q_1$  when simultaneous inputs are applied to the gate and source. The gate is driven by the phase shifter output, while the source input is taken from the phase shifter input via source follower  $Q_2$ . Gain adjustment of the gate voltage is provided by a miniature 10-turn Heli-Trim potentiometer. The differential voltage produced at the  $Q_1$  drain drives a second source follower which provides an output to an external voltmeter. The field effect transistor, a unilateral device, was selected

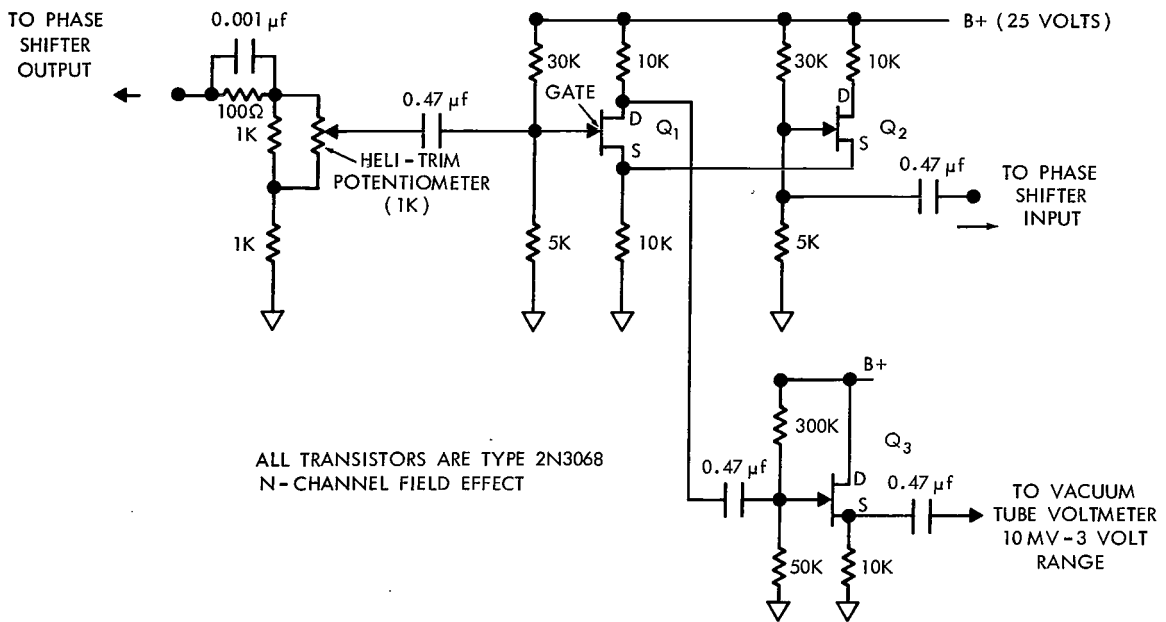


Figure 13—Differential amplifier for indicating zero phase between phase shifter input and output.

because it is necessary that the phase shifter input-output terminals remain electrically isolated. The gain through the phase shifter can be made greater than unity, and self-generated oscillation will occur if isolation is not maintained through the differential amplifier. The principal design requirement for correct indication of phase coincidence is that the gate and source channels introduce equal phase shifts throughout the operating frequency range. The phase shift in the gate channel tends to be larger at the higher frequencies because of the  $Q_1$  gate capacitance to ground. Correction for the difference in capacitance is made with a load network (100 ohms in parallel with  $0.001 \mu f$ ) in the gate circuit of  $Q_1$ . Compensation was achieved over a frequency range from 10 kHz to 700 kHz; imperfect compensation is indicated by a variation in the null with frequency when both inputs are driven from a constant voltage, common source.

## MEASURED PERFORMANCE OF PHASE SHIFTER

### Use of Differential Amplifier for Setting Phase Shifter Zero

As described in the analysis, Line 2 is utilized for linear phase control extending over a 360-degree range. The length of line travelled by the pickup to produce a 360-degree shift in the phase shifter output signal is independent of signal frequency since it involves only the phase shift of the carrier input to the second mixer. However, because of the phase shift in the crystal filter, the zero-phase point on this line would shift with signal frequency at the same rate if line 2 were not provided for compensation. Compensation procedure at any particular signal frequency is to set Line 2 at the zero-phase calibration point; line 1 is then adjusted until a null is observed on the vacuum-tube voltmeter driven by the differential amplifier.

The zero calibration point on line 2 will then correspond to the zero phase of the phase shifter input-output signal. For a minimum null, it will be necessary to adjust the phase shifter output gain control; fine gain adjustment is provided by the 10-turn Heli-Trim potentiometer in the  $Q_1$  gate circuit of the differential amplifier. Imperfect gain adjustment decreases the sensitivity to phase change, but does not cause an error; the null will always correspond to the in-phase condition. Further, nulls occur only at zero degree or integral multiples of 360 degrees (the magnitude of the difference of two equal sine waves is a function of the sine of one-half the relative phase angle). Sensitivity is such that phase coincidence within tenths of degrees is discernible with a vacuum-tube voltmeter having a 10-millivolt scale. Typically with 0.5 volt at the phase shifter input and output terminals, the in-phase null will be 5 mv; a 1-degree phase change from coincidence will produce an increment of 5 mv (double the null value).

Figure 14 plots the Line 1 phase shifter zero calibration versus signal frequency in kHz. The ordinate is plotted in units of the Borg microdial index head attached to the lead screw. The data show that there are as many as three null points on line 1 for each value of signal frequency. Multiple nulls do not constitute an ambiguity since each point corresponds to phase coincidence. The choice of a line 1100 electrical degrees long increases the number of nulls at any given signal frequency but permits the signal frequency range to be covered more nearly continuously. For instance, if locus A in Figure 14 is utilized for a signal frequency range from 230 to 130 kHz, the only lost motion will occur at the 130-kHz reset point where it will be necessary to return to a setting of 260 units (ordinate). Locus B can then be utilized to cover the range from 130 to 30 kHz. If the line were 360 degrees long (the minimum required), the same span in signal frequency could be covered, but lost motion would occur at 3 reset points, 194, 138, and 78 kHz. The zero calibration points shown in Figure 14 will change with the adjustment of the various tuned circuits in the carrier path. Use of the differential amplifier and auxiliary voltmeter for setting the phase shifter zero eliminates the need for recalibration whenever circuit adjustments are made.

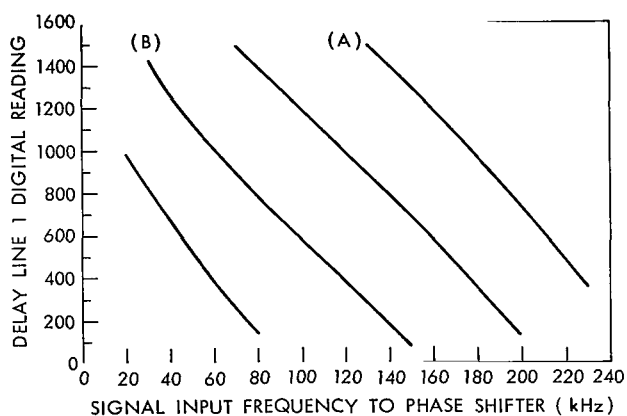


Figure 14—Line 1 setting for phase shifter zero output vs signal frequency.

### Calibration of Line 2 for Continuous Phase Control, 0- to 360-Degree Range

The designated zero point on line 2 is calibrated as previously discussed by adjusting line 1 for a null in the differential amplifier output. Phase shift in a 360-degree range is then obtained by adjustment of line 2. Since the indexing head is not directly calibrated in degrees, such an adjustment to produce a desired phase shift requires that the phase control slope be known. If the line were perfectly linear, no external calibration would be required, since the phase control slope could be determined with the differential amplifier by noting the line index reading corresponding

to the next null on the line; the first null corresponds to zero-degree phase shift, the second to 360 degrees. The control slope could then be calculated by dividing the line index reading by 360. However, since the line is not perfectly linear, calibration with an external phase-indicating instrument is necessary. The calibration procedure will determine the average slope from successive null readings, and then use this slope as the basis for measuring deviation from linearity.

Figure 15 shows the measured phase shifter output phase angle plotted against the lead-screw index reading. Output phase was measured with a commercial phase-indicating instrument in 10-degree increments.

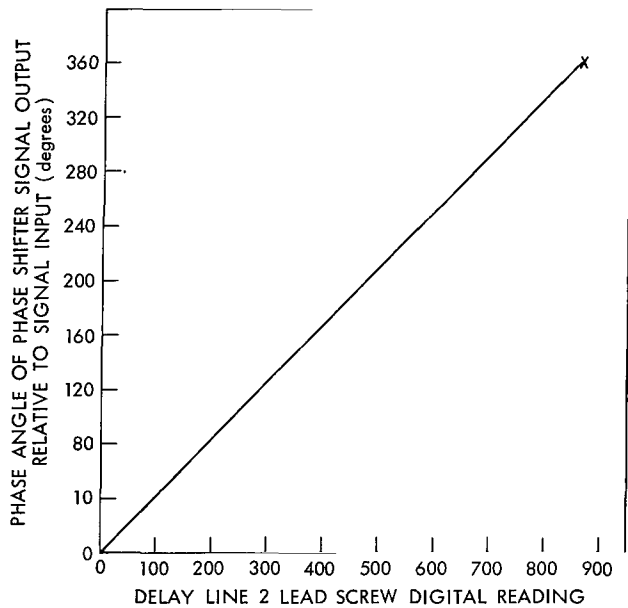


Figure 15—Output signal phase angle vs line 2 lead screw indexing head units (solid line: signal frequency = 100 KHz; x line: signal frequency = 200 kHz).

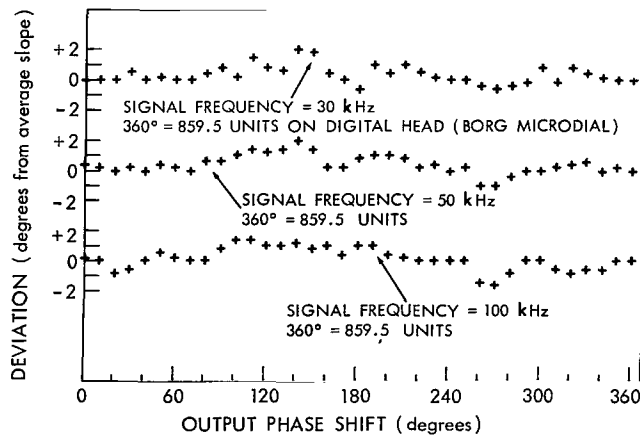


Figure 16—Deviation from linearity in degrees vs output phase angle for signal frequencies of 30, 50, and 100 kHz.

10-degree increments. The conditions were: signal frequency = 100 kHz; signal level = 0.5 volt. The cross at the end point (360 degrees) is the index reading corresponding to the differential amplifier null with a signal frequency of 200 kHz; (phase-meter maximum frequency range = 100 kHz). The scale of the plot does not permit accurate determination of the linearity of the system. More significant data in this regard are shown in Figure 16, where deviations from linearity are plotted against signal frequency. These data were determined from the previous phase measurements plotted to a much larger scale. After the points were plotted, a thread was stretched between the 0-degree and 360-degree points to provide a reference line corresponding to the average slope as determined by the null readings (the nulls coincided with the 0- and 360-degree readings of the phase meter). Deviations relative to this reference line were plotted in Figure 16. Phase deviation at 30 and 50 kHz's is also shown. While these data were taken, the effects of backlash between the lead screw and pickup carriage were minimized by advancing the carriage in a forward direction only. The errors shown are quite consistent and independent of signal frequency as would be expected, since the phase shift is that of the fixed carrier. Repeating the measurements of phase versus the index reading gave the following results at 50 kHz. Of a total of 36 readings, 21 were exactly repeated, 10 showed a deviation from the former reading of 0.2 degree, and 5 showed a deviation from

the former reading of 0.5 degree. The hysteresis resulting from backlash was determined by setting the line to 10-degree intervals read on the phase meter as before, but in the reverse direction (360 to 0 degrees). These readings were then compared to the set obtained when the carriage was moved in the forward direction. The comparison showed an average offset of +1.44 degrees with a standard deviation of  $\pm 0.62$  degree. Thus, the pattern of errors (at 50 kHz) is repeated to within  $\pm 0.62$  degree but with a vertical displacement upwards in Figure 16 of 1.44 degrees. An examination of the pickup carriage during reversal shows a tilting in the direction of motion. The width of the carriage block (0.5 inch) allows only two threads of the lead screw to be engaged. Widening the carriage so as to engage at least four threads would undoubtedly reduce the hysteresis effect.

The causes of the deviations from linearity are not definitely known, particularly as they are related to the uniformity of the delay-line winding. Linearity requires that the inductance of the line be uniformly distributed throughout its length. This calls for constant winding pitch and a uniform diameter with accurate tap spacing. The line is continuously wound with no spacing between turns; thus the pitch would appear to be determined by consistency of the wire diameter. The line was of course initially intended for use with a contact and, as a consequence, the insulation on the line surface adjacent to the carriage block was removed by a grinding process. The effect of this process on the uniformity of distributed inductance is not known.

It was possible to investigate a number of other factors which were considered potential sources of nonlinearity. The following were not considered significant: (1) mechanical linearity of the lead screw, (2) flexure of the coax used for connection to the pickup, (3) line capacitors, (4) termination of the line (a topic which will be considered in the next section), and (5) errors in the phase meter used for calibration. Changes in the electrical environment of the pickup during traverse were then investigated as a source of nonlinearity. Variation of either the inductance of the pickup winding or the capacitance used for resonating produces significant changes in phase shift. If the change is constant, the result is an offset of the phase shifter zero calibration point with no effect on linearity. If the capacitance changes during pickup transit, linearity will be affected. The most critical stray capacitance is between the lower surface of the pickup winding and the main frame bearing plate (Figure 10). The present clearance is about 3/16 inch and might well be increased. However, observation showed that the spacing remained constant during pickup transit, and consequently it was not considered a source of nonlinearity. A second environmental factor considered was the spacing between the toroid gap and line surface. The fiber rod supporting the line winding is not perfectly straight, and variation in spacing occurs during carriage transit. It was determined by moving the line back while observing the output phase shift that the resulting changes in phase were negligible. However, if closer gap-to-line spacing were to be used, this effect could be expected to be a source of nonlinearity.

The last potential source to be considered is the previously mentioned discontinuity noted at the line-to-capacitor junctions. This effect was noted as a small change in pickup output as the pickup passed the turn containing the tap. The observed percentage change in voltage was very small; furthermore, it would be expected to produce a periodic disturbance in phase linearity. Thus it was not considered to account for the observed deviations, which are not periodic.

## Measured Phase Nonlinearity When Line 2 Is Not Terminated in $Z_0$

Figure 17 shows the effect of improper termination of line 2 on phase shifter linearity. Curve 1 is the measured phase shift of the phase shifter output relative to the input versus delay line 2

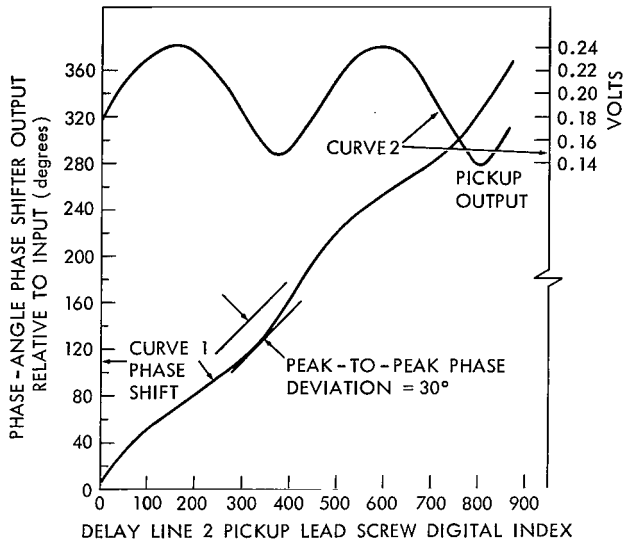


Figure 17—Effect of improper termination of line 2: curve 1, phase shift of output signal (50 kHz) vs pickup traverse; curve 2, amplitude of pickup output vs pickup traverse (terminating impedance =  $287 \text{ H}6.9^\circ$  ohms,  $Z_0 = 453.6 \text{ H}3.5^\circ$  ohms).

pickup lead screw digital reading. The periodic deviation from phase linearity results from deliberately terminating line 2 in an impedance value of  $287 \text{ H}6.9^\circ$  ohms; proper terminating impedance ( $Z_0$ ) is  $453.6 \text{ H}3.5^\circ$  ohms. The signal frequency, 50 kHz, is sufficiently high to eliminate phase nonlinearity which might result from the lower sideband. Improper termination will, of course, also cause the line current as seen by the pickup to vary in a cyclic manner during traverse; this variation is shown by curve 2. Because of the saturation characteristic of the second mixer, whose carrier input is derived from line 2, no variation in the output signal of the phase shifter at 50 kHz was measurable during pickup traverse. Thus the most significant effect of improper termination on phase-shifter operation is the resulting periodic phase deviation. As has been noted in the analysis, the effect of improper termination on phase linearity is identical with the effect produced by the lower

sideband; the magnitude of the former is determined by the reflection factor, and the magnitude of the latter is determined by the sideband ratio. The two effects are distinguishable in that the lower sideband will cause nonlinearity only at the lower signal frequencies and will be accompanied by variation in phase shifter output during pickup traverse.

The maximum deviation from phase linearity shown by curve 1 is of the order of  $\pm 15$  degrees; according to the analysis, the phase deviation can be related to the amplitude fluctuation as follows: From Equation 17, the reflection factor  $R_r$  is related to maximum and minimum amplitude by

$$R_r = \frac{0.242 - 0.147}{0.242 + 0.147} = 0.244$$

where 0.242 and 0.147 are the first maximum and minimum in curve 2. The predicted phase deviation, Equation 17, corresponding to  $R_r = 0.244$  is  $\pm \tan^{-1} 0.244 / \sqrt{1 - (0.244)^2} = \pm 14.11$  degrees. Although the predicted value agrees reasonably well with the measured value of  $\pm 15$  degrees, the reflection factor as calculated from curve 2 is slightly larger than the true value because attenuation of the line current (maximum = -1 db) causes a tilt in the axis of the amplitude fluctuation

plot. Independent calculation of the reflection factor as given by Equation 15 in terms of  $Z_0$  and the load impedance gives a value of 0.225.

Because periodic phase linearity is related to amplitude fluctuation, observation of the pickup output during traverse provides a convenient method for properly terminating the line. This is a fairly tedious process involving trial and error adjustment of four variables, the terminating resistor and inductor and the source resistor and inductor. An X-Y recorder used to make a permanent trace of amplitude fluctuation during pickup traverse is helpful in this process. The Y axis of the recorder can be driven from the ac voltmeter placed across the pickup output; the X axis can be driven simultaneously from a linear time-sweep source. Comparison of traces for each trial set of impedances provides a guide in the selection process. Proper termination for both lines 1 and 2 was determined with this technique.

### Phase Shifter Operating Range in kHz With a 10.580-MHz Carrier Frequency

A frequency of 10.580 MHz places the carrier in the center of the lower band-pass edge of the single sideband filter; the analysis shows this position to be an optimum choice insofar as it permits linear phase shift of the lowest possible signal frequency. The operating range of the phase shifter with this choice of carrier frequency is shown by the data plotted in Figure 18. Phase-shifter output amplitude is plotted versus signal frequency with a constant input level of 0.5 volt. The output signal amplifier gain control was preset for unity system gain at 100 kHz. The resulting amplitude plot form is essentially that of the single sideband filter translated in frequency. These data show that for signal frequencies extending from 30 to 240 kHz, the phase shifter output is free from the effects of the lower sideband; continuous phase control by line 2 will follow the calibration data previously shown in Figures 15 and 16. Above 180 kHz, the decrease in output amplitude results from attenuation of the upper sideband in the single sideband filter; the variation in amplitude in the 40- to 180-kHz region results from ripple in the bandpass region of the filter. Compensation for these effects is provided by the gain control of the output signal amplifier.

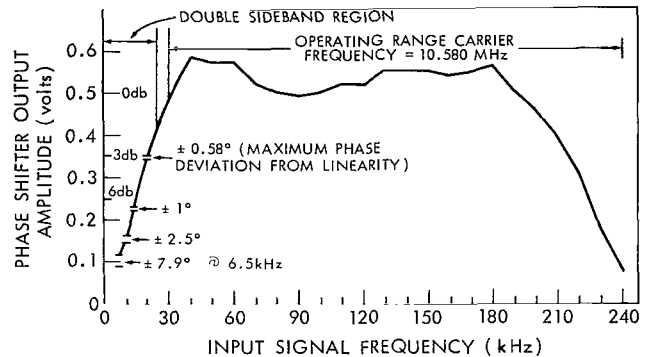


Figure 18—Phase shifter operating range in kHz, output amplitude vs signal frequency with a carrier frequency = 10.580 MHz.

The effects of the lower sideband are evident below signal frequencies of 30 kHz. In this region, the signal output fluctuates in a cyclic manner as the line 2 phase shift is varied. Maximum and minimum amplitude values are indicated by horizontal breaks; these were observed by varying line 2 over a 360-degree range. According to the theory, such cyclic amplitude variation is always accompanied by cyclic phase deviation from linearity, which can be predicted on the basis of the maximum and minimum amplitude values by means of Equations 10 and 11. Calculated

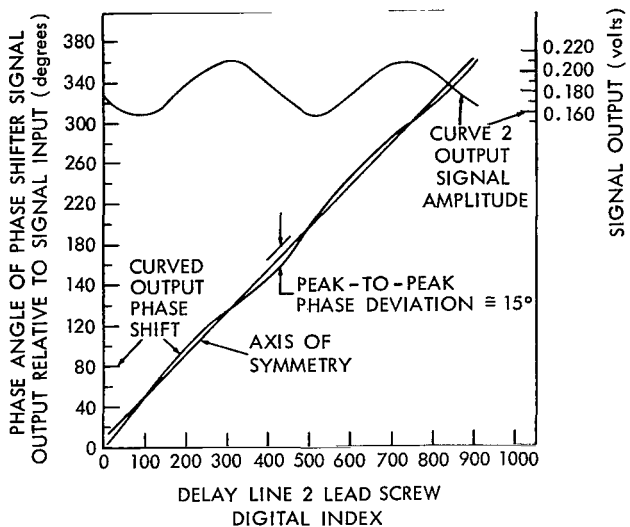


Figure 19—Phase shifter output amplitude and phase vs line 2 pickup traverse with signal frequency = 6.5 KHz.

$$\frac{K_1}{K_2} = \frac{\max - \min}{\max + \min} (\text{amplitude}) = \frac{0.210 - 0.159}{0.210 + 0.159} = 0.138 .$$

(The gain of the output signal amplifier was increased over the setting used for Figure 18 to permit better accuracy.) The maximum and minimum phase deviation predicted by Equation 11 with  $K_1/K_2 = 0.138$  is

$$\pm \tan^{-1} \frac{0.138}{\sqrt{1 - (.138)^2}} = \pm 7.9 \text{ degrees} .$$

According to Equation 9, the phase deviation resulting from the lower sideband is the sum of a linear term  $\theta_x$  and a superimposed arc tangent term with argument  $2\theta_x$ . The linear term  $\theta_x$  establishes the axis of symmetry which passes through values of the sum where the arc tangent term = 0; furthermore, the zero values of the arc tangent terms coincide with the maximum and minimum values of the accompanying amplitude fluctuation. The axis of symmetry was established in the phase plot by noting the position of the maximum and minimum amplitude values of the upper curve. If delay line 1 were set initially so that  $\theta_y = -\xi - \psi$ , the axis of symmetry would intercept the zero point on the abscissa (see the plot of Equation 9, curve D, Figure 3). However, it is difficult to make this setting when the lower sideband is present and the axis of symmetry for the measured data does pass through the zero point on the abscissa.

### Phase Shifter Signal Amplitude Distortion

Amplitude distortion generated by the phase shifter is shown by Figure 20. The upper plot shows the second and third harmonic distortion in decibels relative to the fundamental frequency

phase deviations corresponding to the observed maximum and minimum amplitude values are shown at each break.

This calculation shows that because of an increase in the magnitude of the lower sideband, the deviation from linearity increases from  $\pm 0.5$  degrees at 20 kHz to  $\pm 1$  degree at 14 kHz. The increase is more rapid below 14 kHz. Figure 19 shows the actual measured cyclic phase and amplitude deviation which occurred at 6.5 KHz. Curve 2 is the output amplitude, and curve 1 is the output phase shift. Both are plotted against line 2 microdial readings. The observed value of phase deviation is  $\pm 7.5$  degrees. To predict the phase deviation from the amplitude variation, first determine the sideband ratio from Equation 10:

at 50 kHz. Distortion is plotted for signal levels at the input of 0.3, 0.5, and 1 volt. Distortion levels of the input signal were of the order of -60 db below the fundamental. The lower curve shows distortion at a 200-kHz signal frequency. The lower distortion apparent at this frequency results because the distortion generated by the first mixer is eliminated in the single sideband filter. Distortion in the phase shifter was found to be relatively independent of carrier balance in either mixer. Complete unbalance so as to entirely restore the carrier resulted only in a 3 db increase in second-harmonic distortion with an input signal level of 0.5 volt.

### Effects of Ambient Temperature Variation, 65° to 90°F

Variation of temperature in the range 65° to 90°F causes a shift in the output phase of approximately 2 degrees in the 86° region. In practice, such a change would require resetting the phase shifter zero calibration point by means of the differential-amplifier technique. Other than the shift in zero, the phase calibration of line 2 in a 360-degree range was found to be unchanged by the temperature variation in the interval cited. Figure 21 shows the measured phase of the phase shifter output signal versus temperature. Initial setting of the phase shifter zero phase output was made at 76°F. The phase readings are values obtained after temperature equilibrium in a temperature-controlled oven. The response time required to reach equilibrium after a 10° temperature change was of the order of 45 minutes. Transient phase deviation before equilibrium was reached did not exceed 3 degrees; this transient deviation was presumably due to a temperature difference in the various phase shifter components.

The most critical components with respect to temperature are the ferrite toroids in the pickups. The change of permeability of the cores is of the order of 0.1 percent per °C (without air gap). However, the pickups are in alternate carrier channels, with the result that the net phase change is the difference between the phase change produced by each pickup. In order to achieve the relatively flat characteristic shown by Figure 21, it was necessary to optimize the cancellation between pickups by installing a compensating capacitor with a negative 750-parts-per-million temperature coefficient in parallel with the line 1 pickup tuning capacitor. Compensation for temperature was not difficult, since the phase variation with temperature tends to be quite linear.

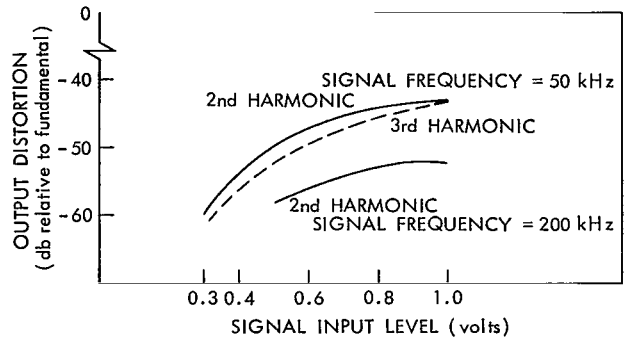


Figure 20—Phase shifter signal distortion vs signal level.

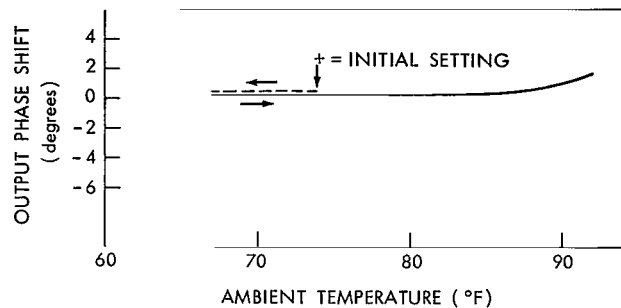


Figure 21—Phase shifter vs ambient temperature with signal frequency = 50 kHz.

## Phase Shifter Operating Range in kHz With a 10.258-MHz Carrier Frequency

The frequency of the upper sideband must lie within the fixed bandpass of the single sideband filter throughout the operating range of the phase shifter. Because the signal frequency corresponds to the difference between the upper sideband and carrier frequency, lowering the carrier

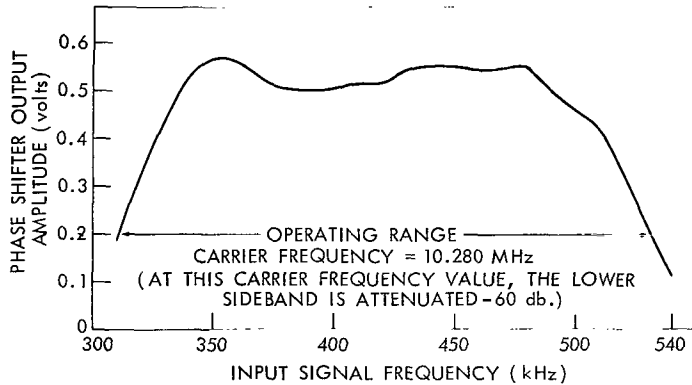


Figure 22—Phase shifter operating range with carrier frequency lowered 300 kHz to 10.280 MHz (phase shifter output amplitude is plotted against signal frequency).

frequency shifts the operating range upwards. Figure 22 shows the resulting operating range when the carrier frequency is lowered 300 kHz to 10.258 MHz. Output amplitude is plotted versus input signal frequency with a single input of 0.5 volt. The output signal amplifier gain control was preset for unity gain at 400 kHz. The plot profile is identical with the plot profile corresponding to a carrier frequency of 10.580 MHz (Figure 18) except for a translation in frequency. The circuit adjustments required for the change in carrier frequency were slight retuning of the carrier amplifier tank capacitors and the pickup tuning capaci-

tors; both mixers were then rebalanced for carrier rejection. Termination of the delay lines was not affected by the change. Measurement of the line outputs (amplitude versus pickup position) indicate no deterioration in phase linearity from reflections. The data show that the operating range extends from 310 to 540 kHz; the lower region to the left is free from the effects of the lower sideband, which is attenuated by at least -60 db in the single sideband filter. (At this value of carrier frequency, the lower sideband lies 570 kHz below the frequency corresponding to -60 db in the single sideband filter.) Operating procedures remain unchanged. At any particular frequency, line 2 is set on the zero-phase calibration point and line 1 is adjusted for phase coincidence by noting the null on the meter driven by the differential amplifier. Line 2 can then be set for any desired phase shift. Since the carrier frequency is lower, both lines will appear electrically longer. With the lower carrier frequency value, the digital calibration for line 2 is 0.4067 degree per dial reading digit (360 degrees = 885 units).

## CONCLUSIONS

The use of an inductive delay line pickup in a heterodyne phase shifter circuit has been shown to provide variable phase shift with infinite resolution. Reliability of the system is high, since variable phase shift is obtained without the use of sliding contacts or range-changing switches. The heterodyne method phase-shifts an input sine wave indirectly by phase-shifting a fixed frequency carrier. Several advantages of this indirect technique were demonstrated. Calibration errors are independent of the frequency of the input signal. The frequency range of the system can be changed

easily by shifting the carrier frequency; the technique, however, is not suitable for very low values of signal frequency. Phase shift is provided over a 360-degree range without attendant amplitude variation. Circuitry is straightforward without the use of complicated networks. Measurements showed close agreement with values predicted by analysis.

Goddard Space Flight Center  
National Aeronautics and Space Administration  
Greenbelt, Maryland, December 20, 1966  
125-21-02-01-51

#### REFERENCES

1. Pappenfus, E. W., "Single Sideband Principles and Circuits," p. 53, New York: McGraw-Hill, 1964.
2. Geffe, P. R., "Simplified Modern Filter Design," New York: John F. Rider, 1963.
3. Guillemin, E. A., "Communication Networks," Vol. II, pp. 41-47, New York: John Wiley, 1935.
4. Terman, F. E., "Radio Engineering," p. 53, Third Edition, New York: McGraw-Hill, 1947.
5. Ramo, S., and Whinnery, J. R., "Fields and Waves in Modern Radio," pp. 215-228, Second Edition, New York: John Wiley, 1962.



## Appendix A

### Partial List of Symbols

<u>Symbol</u>	<u>Meaning</u>
$C_1, C_2$	Distributed capacitance for line 1 and line 2, respectively
$E_c$	Peak amplitude of carrier
$E_s$	Peak amplitude of signal
$K_1$	Amplitude coefficient of single sideband filter applied to lower sideband
$K_2$	Amplitude coefficient of single sideband filter applied to upper sideband
$L_1, L_2$	Distributed inductance for line 1 and line 2, respectively
$R_r$	Delay-line reflection factor
$x$	Distance from line 2 input to center of pickup gap
$y$	Distance from line 1 input to center of pickup gap
$Z_0$	Characteristic impedance of delay line
$Z_r$	Terminating impedance of delay line
$\theta_x$	Phase angle introduced to carrier by line 2
$\theta_y$	Phase angle introduced to carrier by line 1
$\xi$	Phase angle introduced to carrier by single sideband filter
$\phi$	Phase angle of reflection factor $R_r$
$\psi$	Differential phase angle relative to carrier phase angle $\xi$ , introduced to upper and lower side band by single sideband filter
$\omega_c$	Radian frequency of carrier
$\omega_s$	Radian frequency of signal



## Appendix B

### Effect of Lower Sideband on Phase Shifter Output

The phase shifter output with both sidebands consists of two terms given by Equation 4:

$$\frac{E_s}{12} \left[ K_1 \sin(\omega_s t + \xi - \psi + \theta_y - \theta_x) + K_2 \sin(\omega_s t - \xi - \psi - \theta_y + \theta_x) \right] . \quad (B1)$$

For any signal frequency  $\omega_s$ , let delay line 1 be adjusted so that

$$-\xi - \psi = \theta_y .$$

Then Equation B1 reduces to

$$\frac{E_s}{12} \left[ K_1 \sin(\omega_s t - 2\psi - \theta_x) + K_2 \sin(\omega_s t + \theta_x) \right] . \quad (B2)$$

The analysis is made much simpler if the above expression is converted to the following exponential equivalent:\*

$$\frac{E_s}{12} I_M \left[ K_1 e^{j(\omega_s t - 2\psi - \theta_x)} + K_2 e^{j(\omega_s t + \theta_x)} \right] . \quad (B3)$$

Factor out the  $K_2 e^{j(\omega_s t + \theta_x)}$  term:

$$\frac{E_s}{12} I_M \left[ K_2 e^{j(\omega_s t + \theta_x)} \left( 1 + \frac{K_1}{K_2} e^{-2j(\theta_x + \psi)} \right) \right] . \quad (B4)$$

\* $Ae^{jx} = A(\cos x + j \sin x)$ ;  $I_M[Ae^{jx}] = A \sin x$ , where  $I_M$  is "Imaginary part of."

To clear the above expression, it is necessary to convert  $1 + K_1/K_2 e^{-2j(\theta_x + \psi)}$  to exponential form:

$$\begin{aligned}
1 + \frac{K_1}{K_2} e^{-2j(\theta_x + \psi)} &= 1 + \left(\frac{K_1}{K_2}\right) \cos(2\theta_x + 2\psi) - j \left(\frac{K_1}{K_2}\right) \sin(2\theta_x + 2\psi) \\
&= \left[1 + \frac{K_1^2}{K_2^2} + 2 \left(\frac{K_1}{K_2}\right) \cos(2\theta_x + 2\psi)\right]^{1/2} \exp \left[ -j \tan^{-1} \left( \frac{\left(\frac{K_1}{K_2}\right) \sin(2\theta_x + 2\psi)}{1 + \left(\frac{K_1}{K_2}\right) \cos(2\theta_x + 2\psi)} \right) \right] \dots \quad (B5)
\end{aligned}$$

Substitute Equation B5 in B4:

$$\frac{E_s}{12} I_M \left\{ K_2 \left[1 + \frac{K_1^2}{K_2^2} + 2 \frac{K_1}{K_2} \cos(2\theta_x + 2\psi)\right]^{1/2} \exp \left[ +j \left( \omega_s t + \theta_x - \tan^{-1} \frac{\left(\frac{K_1}{K_2}\right) \sin(2\theta_x + 2\psi)}{1 + \left(\frac{K_1}{K_2}\right) \cos(2\theta_x + 2\psi)} \right) \right] \right\} \quad (B6)$$

The imaginary part of this expression is the desired result:

$$\frac{E_s}{12} K_2 \left[1 + \frac{K_1^2}{K_2^2} + 2 \frac{K_1}{K_2} \cos(2\theta_x + 2\psi)\right]^{1/2} \sin \left( \omega_s t + \theta_x - \tan^{-1} \frac{\left(\frac{K_1}{K_2}\right) \sin(2\theta_x + 2\psi)}{1 + \left(\frac{K_1}{K_2}\right) \cos(2\theta_x + 2\psi)} \right) \quad (B7)$$

The presence of the lower sideband thus results in amplitude variation and an arc tan phase perturbation, both of which are functions of  $2\theta_x$ . The arc tan perturbation term is plotted in Figure D1, Appendix D in the general form  $\tan^{-1} F \sin W / (1 + F \cos W)$  (the function is also applicable to the delay line); in this case,  $F = K_1/K_2$  and,  $W = 2\theta_x + 2\psi$ . It is a periodic function which alters shape radically with the parameter  $K_1/K_2$ , being quasi sinusoidal for  $K_1/K_2 \leq 0.2$  and triangular for  $K_1/K_2 = 1$ . It shows a well defined maximum and minimum value which occur for values of the argument,  $2\theta_x + 2\psi$  given by the relationship  $\cos(2\theta_x + 2\psi) = -K_1/K_2$ . The maximum or minimum value in degrees is

$$\tan^{-1} \frac{\frac{K_1}{K_2}}{\left[1 - \left(\frac{K_1}{K_2}\right)^2\right]^{1/2}} \quad (B8)$$

The periodic amplitude factor involving the cosine (Equation B7) also shows a maximum or minimum which is expressible in terms of the sideband ratio  $K_1/K_2$ . The maximum occurs

when  $\cos(2\theta_x + 2\psi) = 1$  and is

$$\frac{E_s}{12} K_2 \left[ 1 + 2 \frac{K_1}{K_2} + \left( \frac{K_1}{K_2} \right)^2 \right]^{1/2} = + \frac{E_s}{12} K_2 \left( 1 + \frac{K_1}{K_2} \right) .$$

The minimum amplitude occurs when  $\cos(2\theta_x + 2\psi) = -1$ , and is

$$\frac{E_s}{12} K_2 \left[ 1 - 2 \frac{K_1}{K_2} + \left( \frac{K_1}{K_2} \right)^2 \right]^{1/2} = + \frac{E_s}{12} K_2 \left( 1 - \frac{K_1}{K_2} \right) .$$

The ratio of maximum to minimum amplitude can be written

$$\frac{\max}{\min} = \frac{1 + \frac{K_1}{K_2}}{1 - \frac{K_1}{K_2}} .$$

This can be solved to give the relationship

$$\frac{K_1}{K_2} = \frac{\max - \min}{\max + \min} \text{ (phase shifter output amplitude) .} \quad (\text{B9})$$

Two additional relations between the cosine amplitude term of Equation B7 and the arc tan phase terms can be derived. The first relationship is that the zero values of the arc tan term occur when the amplitude is a maximum or minimum. The zero of the arc tan term requires that the numerator in its argument be zero;  $\sin(2\theta_x + 2\psi) = 0$  thus  $(2\theta_x + 2\psi) = 0, \pi, 2\pi$ . The cosine term in the amplitude function will be  $\cos 0 = 1$  (maximum amplitude);  $\cos \pi = -1$  (minimum amplitude);  $\cos 2\pi = +1$  (maximum amplitude). The second relationship is that the value of the amplitude function corresponding to the maximum and minimum values of the arc tan term is given by  $\sqrt{\max \cdot \min}$  (amplitude). From Appendix D, Equation D2, the maximum and minimum of the arc tan occurs when  $\cos(2\theta_x + 2\psi) = -K_1/K_2$ . Substitution of this relationship in the amplitude function, B7 gives

$$\begin{aligned} K_2 \frac{E_s}{12} \left( 1 + \frac{K_1^2}{K_2^2} - 2 \frac{K_1}{K_2} \right)^{1/2} &= \frac{E_s}{12} K_2 \left( 1 - \frac{K_1^2}{K_2^2} \right)^{1/2} = \frac{E_s}{12} K_2 \sqrt{1 - \frac{K_1}{K_2}} \cdot \sqrt{1 + \frac{K_1}{K_2}} \\ &= \sqrt{\max \cdot \min} \text{ (amplitude)} \\ &= \text{value of amplitude when arc tan term is either} \\ &\quad \text{maximum or minimum .} \end{aligned} \quad (\text{B10})$$



## Appendix C

### Distributed Constant Delay Line With Toroidal Pickup

In order to determine the pickup output for a configuration as shown by Figure C1, it is first necessary to determine the current distribution along the line. Consider the schematic of a uniformly distributed constant delay line without the pickup (Figure C1). With the reference point placed at the input to the line ( $z = 0$ ) the current  $i(z, t)$  at any point  $z$  is (Reference 3)

$$\text{IM} \left[ e^{j\omega_c t} \bar{I}(z) \right] , \quad (\text{C1})$$

where

$$\bar{I}(z) = \frac{E_c \left[ (\bar{Z}_r + \bar{Z}_0) e^{a(\ell-z)} - (\bar{Z}_r - \bar{Z}_0) e^{-a(\ell-z)} \right]}{(\bar{Z}_s + \bar{Z}_0) (\bar{Z}_r + \bar{Z}_0) e^{a\ell} - (\bar{Z}_s - \bar{Z}_0) (\bar{Z}_r - \bar{Z}_0) e^{-a\ell}} . \quad (\text{C2})$$

- $\bar{Z}_s$  = Internal impedance of generator,
- $\bar{Z}_0$  = characteristic impedance of line,
- $\bar{Z}_r$  = terminating impedance,
- $a$  = propagation constant of line,
- $\ell$  = line length,
- IM = "imaginary part of."

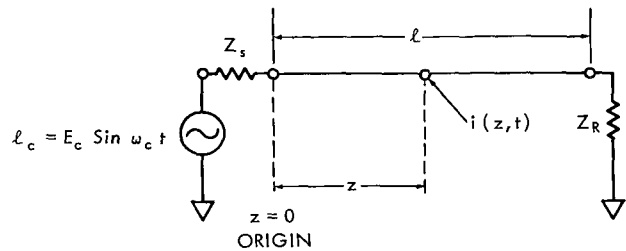


Figure C1—Transmission line schematic without pickup.

The further development of Equation C2 is generally familiar, but is not usually in the form desired here; the phase perturbation resulting from an improperly terminated line is seldom shown in detail. The phase and amplitude of the current at any point on the line will be determined for the case of the lossless line with the generator impedance equal to  $Z_0$ ,  $Z_s = Z_0$ . With this current known the output of the toroidal pickup can be determined. For the case of the lossless line, the propagation constant  $\alpha = j\omega_c \sqrt{LC} = j\beta$  where  $L$  = inductance per unit of line length,  $C$  = capacitance per unit of line length. With this relationship and  $Z_s = Z_0$ , Equation C2 reduces to

$$\bar{I}(z) = \frac{E_c}{2Z_0} e^{-j\beta\ell} \left[ e^{j\beta(\ell-z)} - \frac{\bar{Z}_r - Z_0}{\bar{Z}_r + Z_0} e^{-j\beta(\ell-z)} \right] . \quad (\text{C3})$$

The factor  $(\bar{Z}_r - Z_0)/(\bar{Z}_r + Z_0)$ , termed the reflection coefficient will be expressed in polar form as  $R_r e^{j\phi}$ ; substitute this latter definition in Equation C3 and multiply through by  $e^{-j\beta\ell}$ :

$$\bar{I}(z) = \frac{E_c}{2Z_0} \left[ e^{-j\beta z} - R_r e^{j(\beta z - 2\beta\ell + \phi)} \right] . \quad (C4)$$

Factor out  $e^{-j\beta z}$ :

$$\bar{I}(z) = \frac{E_c}{2Z_0} e^{-j\beta z} \left[ 1 - R_r e^{j(2\beta z - 2\beta\ell + \phi)} \right] . \quad (C5)$$

Note that because  $Z_0 = \sqrt{L/C}$ ,  $Z_0$  is purely resistive in the case of the lossless line, the symbol for  $Z_0$  is written without the bar. For latter application, it is desirable to alter the minus sign preceding the  $R_r$  term in Equation C5. Use the relationship  $e^{j\pi} = -1$ :

$$\bar{I}(z) = \frac{E_c}{2Z_0} e^{-j\beta z} \left[ 1 + R_r e^{j(2\beta z - 2\beta\ell + \phi + \pi)} \right] . \quad (C6)$$

The expression in the brackets is converted to polar form as follows. Let  $(2\beta z - 2\beta\ell + \phi + \pi) = \lambda$ :

$$\begin{aligned} 1 + R_r e^{j\lambda} &= (1 + R_r \cos \lambda) + j R_r \sin \lambda \\ &= \left[ 1 + 2R_r \cos \lambda + R_r^2 \right]^{1/2} \exp \left[ j \tan^{-1} \frac{R_r \sin \lambda}{1 + R_r \cos \lambda} \right] . \end{aligned}$$

Substitute the above exponential form in Equation C6:

$$\bar{I}(z) = \frac{E_c}{2Z_0} \left[ 1 + 2R_r \cos \lambda + R_r^2 \right]^{1/2} \exp \left[ -j \left( \beta z - \tan^{-1} \frac{R_r \sin \lambda}{1 + R_r \cos \lambda} \right) \right] . \quad (C7)$$

Finally, with this expression substituted in Equation C1, the current at a point  $z$  is

$$i(z, t) = \frac{E_c}{2Z_0} \left( 1 + 2R_r \cos \lambda + R_r^2 \right)^{1/2} \sin \left( \omega_c t - \beta z + \tan^{-1} \frac{R_r \sin \lambda}{1 + R_r \cos \lambda} \right) . \quad (C8)$$

From Equation C8 the current magnitude will vary periodically with  $z$ . Also, the output phase shift will be subject to a perturbation component superimposed on the linear phase shift term  $\beta z$ . These effects are of course reduced to zero for a line terminated in  $Z_0$ , for then  $R_r = 0$ . In this

case,

$$i(z, t) = \frac{E_c}{2Z_0} \sin(\omega_c t - \beta z) \quad . \quad (C9)$$

Since it is difficult to achieve this condition perfectly, it is desirable to determine how much the linearity of phase shift is effected by  $R_r$ . The phase shift perturbation term (Equation C8) is of the form  $\tan^{-1} F \sin W / (1 + F \cos W)$  which has been plotted in Appendix D, Figure D1. In this case  $F = W$  and  $W = 2\beta z - 2\beta l + \phi + \pi$ . The absolute value of the maximum or minimum of this function is a measure of the maximum deviation from linearity to be expected in the phase shifter output. This maximum or minimum is shown to be  $\tan^{-1} R_r / \sqrt{1 - R_r^2}$ . The variation of the amplitude of  $i(z, t)$  attendant with the phase perturbation is of less consequence to the operation of the phase shifter because of the limiting action of the mixers. However, the maximum and minimum values of amplitude are of use in predicting the phase deviation, since the value of  $R_r$  is related to these values: Maximum or minimum amplitude occurs when  $\cos(2\beta z - 2\beta l + \phi + \pi) = \pm 1$ . Thus  $i(z, t)_{\max} = \sqrt{1 + 2R_r + R_r^2} = 1 + R_r$  and  $i(z, t)_{\min} = \sqrt{1 - 2R_r + R_r^2} = 1 - R_r$ . The ratio of  $i(z, t)_{\max}$  to  $i(z, t)_{\min}$ , termed the current standing-wave ratio, is

$$\frac{i(z, t)_{\max}}{i(z, t)_{\min}} = \frac{1 + R_r}{1 - R_r} \quad .$$

This equation can be solved for  $R_r$  to give the useful relationship

$$\frac{i(z, t)_{\max} - i(z, t)_{\min}}{i(z, t)_{\max} + i(z, t)_{\min}} = R_r \quad . \quad (C10)$$

With the current determined relative to the input point on the line, consider the pickup and line configuration shown by Part A of Figure C2. To expedite the analysis which follows, the reference point has been shifted to the center of the pickup gap. The line current with respect to the new coordinate system is  $i(z_0 + z', t)$ , where the line input point is now  $z_0$  units to the left of the new origin and  $z'$  is the variable in the new coordinate system. The pickup distance  $d$  normal from the line is considered to be sufficiently small to make the distance from the center of the gap to any point on the line a small fraction of the wavelength in free space of the carrier generator frequency; from the geometry of the system, this distance is  $\sqrt{d^2 + (z')^2}$ . The coupling mechanism between the line and the toroid is assumed to be a distributed mutual inductance parameter  $M(z')$  associated with each element of line current. Because of the small spacing,  $M(z')$  is assumed to be independent of frequency. In essence, the pickup and line are considered to be a transformer with a section of line adjacent to the pickup forming the primary, while the toroidal winding forms the secondary. The pickup output will be derived for two cases: (1)  $M(z')$  is an even-valued function ( $M(z') = M(-z')$ ), (2)  $M(z')$  is not an even-valued function ( $M(z') \neq M(-z')$ ).

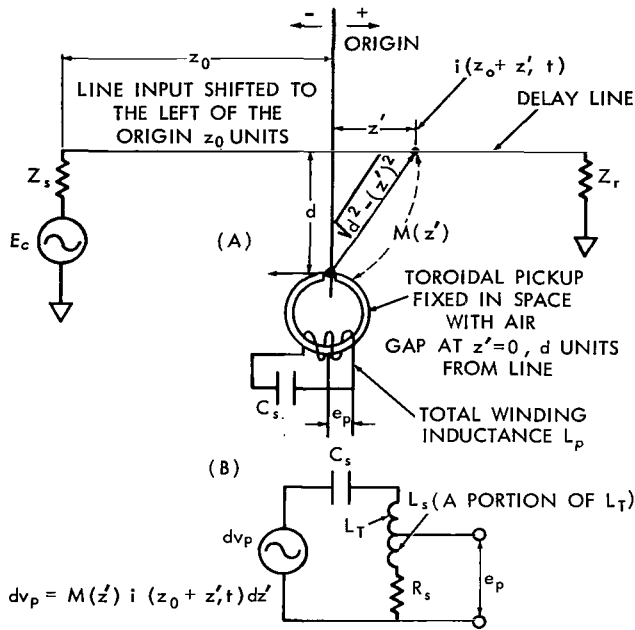


Figure C2—Schematic used for analysis of inductive pickup.

Case 1 will be considered first. It will be shown that if the mutual inductance parameter  $M(z')$  is an even-valued function, the pickup output voltage is equal to the line current at the origin multiplied by an amplitude factor which is a constant. The voltage induced in the secondary of a transformer with primary current  $I_p$  is  $-j\omega M I_p$ , where  $M$  is the mutual inductance (Reference 4). In the case of the line and pickup, induced voltage in the pickup resulting from a section of line  $dz'$  is

$$dV_p = -j\omega_c M(z') i(z_0 + z', t) dz' . \quad (C11)$$

For Part B of Figure C2, let the coil inductance  $L_T$  be resonated by  $C_s$ ; the current in the coil  $di_s$  resulting from  $dV_p$  is  $dV_p/R_s$ . With the above relationship, this gives

$$di_s = \frac{-j\omega_c M(z') i(z_0 + z', t)}{R_s} dz' . \quad (C12)$$

The open circuit pickup voltage  $de_p$  taken across the inductive tap  $L_s$ , is  $j\omega_c L_s di_s$ , assuming the distributed resistance of the tap to be small relative to  $L_s$ . With the value of current given by Equation C12, this voltage can be written as

$$de_p = \frac{\omega_c^2 L_s M(z') i(z_0 + z', t)}{R_s} dz' . \quad (C13)$$

The total voltage induced in the pickup for an inductance function distributed from  $z' = -F$  to  $z' = F$  is

$$e_p = \frac{\omega_c^2 L_s}{R_s} \int_{-F}^F M(z') i(z_0 + z', t) dz' . \quad (C14)$$

Next, consider the expression  $i(z_0 + z', t)$  in the integrand of Equation C14. If the loading of the pickup is neglected the line current  $i(z_0 + z', t)$  can be obtained by substituting Equation C4 in Equation C1. But it will be necessary to rewrite these expressions with respect to the new coordinate system: Let  $z = z_0 + z'$  in Equation C4 and substitute the resulting expression  $\bar{I}(z_0 + z')$

in Equation C1 to give  $i(z_0 + z', t)$ :

$$i(z_0 + z', t) = \frac{E_c}{2Z_0} \text{IM} \left( e^{j\omega_c t} \left[ e^{-j\beta z_0} \times e^{-j\beta z'} - R_r e^{j(\beta z_0 - 2\beta \ell + \phi)} \times e^{j\beta z'} \right] \right) \quad (C15)$$

Rewrite the exponential portion of Equation C15 using the identity\*

$$\text{IM}(e^{ja} \times e^{jb}) \equiv \text{IM} e^{ja} \times \text{RE} e^{jb} + \text{RE} e^{ja} \times \text{IM} e^{jb} \quad .$$

Thus,

$$\begin{aligned} & \text{IM} \left( e^{j(\omega_c t - \beta z_0)} \times e^{-j\beta z'} - R_r e^{j(\omega_c t + \beta z_0 - 2\beta \ell + \phi)} \times e^{j\beta z'} \right) \\ & \equiv \text{IM} e^{j(\omega_c t - \beta z_0)} \text{RE} e^{-j\beta z'} + \text{RE} e^{j(\omega_c t - \beta z_0)} \times \text{IM} e^{-j\beta z'} \\ & \quad - R_r \left( \text{IM} e^{j(\omega_c t + \beta z_0 - 2\beta \ell + \phi)} \times \text{RE} e^{j\beta z'} + \text{RE} e^{j(\omega_c t + \beta z_0 - 2\beta \ell + \phi)} \times \text{IM} e^{j\beta z'} \right) \quad (C16) \end{aligned}$$

After Equation C16 is multiplied by the factor  $E_c/2Z_0$ , the resultant expression for  $i(z_0 + z', t)$  is now in suitable form for integration with respect to  $z'$ . Substitute the resultant expression for  $i(z_0 + z', t)$  in Equation C14 to determine the pickup output:

$$\begin{aligned} e_p &= \frac{\omega_c^2 L_s E_c}{2Z_0 R_s} \left[ \text{IM} e^{j(\omega_c t - \beta z_0)} \times \int_{-F}^F M(z') \cos(\beta z') dz' - \text{RE} e^{j(\omega_c t - \beta z_0)} \times \int_{-F}^F M(z') \sin(\beta z') dz' \right. \\ & \quad - R_r \text{IM} e^{j(\omega_c t + \beta z_0 - 2\beta \ell + \phi)} \times \int_{-F}^F M(z') \cos(\beta z') dz' \\ & \quad \left. - R_r \text{RE} e^{j(\omega_c t + \beta z_0 - 2\beta \ell + \phi)} \times \int_{-F}^F M(z') \sin(\beta z') dz' \right] \quad (C17) \end{aligned}$$

But if  $M(z')$  is an even function, the integral

$$\int_{-F}^F M(z') \sin(\beta z') dz' = 0$$

\*Exponential form of the identity  $\sin(a + b) (\equiv \sin a \cos b + \cos a \sin b)$ . RE = Real part of.

because the integrand is the product of an even function,  $M(z')$ , and an odd function,  $\sin(\beta z')$ , integrated over equal positive and negative intervals. Consequently Equation C17 reduces to

$$e_p = \frac{\omega_c^2 L_s}{R_s} \int_{-F}^F M(z') \cos(\beta z') dz' \cdot \text{IM} \left\{ \frac{E_c}{2Z_0} e^{j\omega_c t} \left( e^{-j\beta z_0} - R_r e^{j(\beta z_0 - 2\beta l + \phi)} \right) \right\} . \quad (\text{C18})$$

*expression for line current at the origin*

The expression on the right of Equation C18 is the expression for the line current,  $i(z_0, t)$ , at the origin opposite the pickup gap. The pickup output is this current multiplied by an amplitude factor. Since the geometry determining  $M(z')$  (part of the amplitude factor) does not change with  $z_0$ , the expression for pickup output could be expected to be valid for any particular value of  $z_0$ , (provided that the pickup is not moved too close to either end of the line). Using the type of reduction shown by Equations C4 through C8, the pickup output can be written without exponentials as

$$e_p = \left[ \frac{\omega_c^2 L_s E_c}{2Z_0 R_s} \int_{-F}^F \cos(\beta z') M(z') dz' \right] (1 + R_r \cos \lambda + R_r^2)^{1/2} \cdot \sin \left( \omega_c t - \beta z_0 + \tan^{-1} \frac{R_r \sin \lambda}{1 + R_r \cos \lambda} \right) , \quad (\text{C19})$$

where

$$\lambda = 2\beta z_0 - 2\beta l + \phi + \pi, \text{ and}$$

$z_0 =$  distance from line input to center of pickup gap.

If the reflection factor  $R_r = 0$ , the pickup output voltage is

$$e_p = \frac{\omega_c^2 L_s E_c}{2Z_0 R_s} \int_{-F}^F \cos(\beta z') M(z') dz' \cdot \sin(\omega_c t - \beta z_0) . \quad (\text{C20})$$

The reflection factor  $R_r$  in terms of the maximum and minimum pickup output voltage measured during pickup if the line is improperly terminated (i.e.  $Z_r \neq Z_0$ ) is

$$R_r = \frac{e_p(\text{max}) - e_p(\text{min})}{e_p(\text{max}) + e_p(\text{min})} . \quad (\text{C21})$$

For case II, the integral

$$\int_{-F}^F \sin(\beta z') M(z') dz' .$$

will not be zero because  $M(z') \neq M(-z')$ . The reduction of Equation 17 with this condition can be made with the techniques previously shown. If  $M(z') \neq M(-z')$  the pickup output is

$$e_p = \frac{\omega_c^2 L_s E_c}{2Z_0 R_s} \sqrt{C_1^2 + C_2^2} \sqrt{1 + 2R_r \cos \lambda' + R_r^2} \sin \left( \omega_c t - \beta z_0 - \tan^{-1} \left( \frac{C_2}{C_1} \right) + \tan^{-1} \frac{R_r \sin \lambda'}{1 + R_r \cos \lambda'} \right) \quad , \quad (C22)$$

where

$$C_2 = \int_{-F}^F M(z') \sin(\beta z') dz' \quad ,$$

$$C_1 = \int_{-F}^F M(z') \cos(\beta z') dz' \quad ,$$

$$\lambda' = \lambda + 2 \tan^{-1} \left( \frac{C_2}{C_1} \right) \quad .$$

An examination of this equation leads to the conclusion that the effects of  $M(z')$  being odd-valued are to modify the amplitude factor and to add a phase angle to the pickup output. Neither effect is significant because the terms involved are constants. Equation C19 is quoted in the text, as  $M(z')$  is considered most likely to be even-valued, since  $M(z')$  could be expected to vary inversely with distance (Reference 5)—in this case, the distance between any point on the line and the center of the pickup air gap. This distance  $\sqrt{d^2 + (z')^2}$  is an even-valued function of  $z'$ . A restatement of assumptions is listed below:

- (1) The delay line is lossless with distributed constants.
- (2) The generator driving the line is matched to the line.
- (3) The pickup is coupled to the line via mutual inductance which is a geometric parameter, not a function of frequency.
- (4) The mutual inductance is an even-valued function of  $z'$  over an interval from  $z' = -F$  to  $z' = F$ , and is zero outside this interval.
- (5) The presence of the pickup does not alter the current in the delay line.



## Appendix D

### Phase Function $\tan^{-1} F \sin W / (1 + F \cos W)$

A periodic phase perturbation of identical shape results in the phase-shifter output if either the lower sideband is present, or if the carrier delay lines are not properly terminated. This perturbation term is of the form  $\tan^{-1} F \sin W / (1 + F \cos W)$ . Because this function can not be reduced further, a plot was made, Figure D1, to illustrate its peculiar characteristics. Four curves were plotted, each corresponding to a separate value of F. This plot shows that the function undergoes a drastic alteration in shape as  $F \rightarrow 1$ . The maximum or minimum value of this function in terms of the parameter F is important to the design of the phase shifter; it is given by first setting the derivative = 0:

$$\frac{d}{dW} \left( \tan^{-1} \frac{F \sin W}{1 + F \cos W} \right) = \frac{F \cos W + F^2}{1 + 2F \cos W + F^2} = 0 \quad (D1)$$

If the value  $F = 1$  is excluded, the zero corresponds to the zero of the numerator;  $F \cos W + F^2 = 0$ . Thus the maximum or minimum value occurs for a value of W given by

$$\cos W = -F \quad (D2)$$

This relationship is then substituted in the original arc tan expression to give the maximum or minimum:

$$\begin{aligned} \text{Max or Min value of } \tan^{-1} \frac{F \sin W}{1 + F \cos W} \\ = \tan^{-1} \frac{\pm F}{(1 - F^2)^{1/2}} = \pm \tan^{-1} \frac{F}{(1 - F^2)^{1/2}} \quad (D3) \end{aligned}$$

where  $F < 1$ . The plot, Figure D1, shows the maximum value corresponds to positive sign, the negative sign to the minimum.

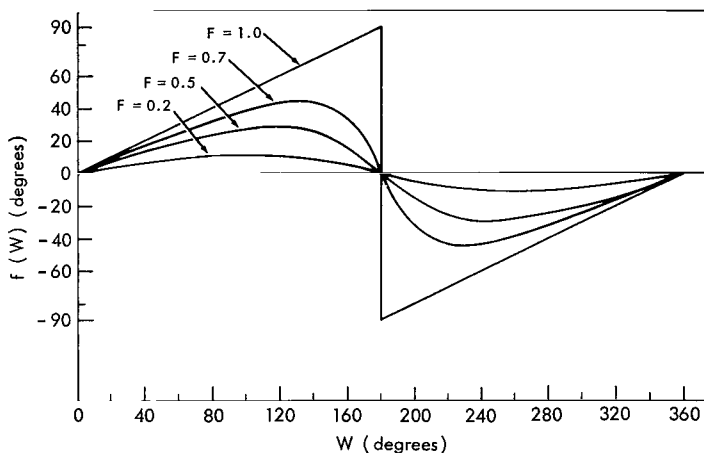


Figure D1—Plot of  $f(W) = \tan^{-1} F \sin W / (1 + F \cos W)$ ,  $F = 0.2, 0.5, 0.7, 1.0$ .

*"The aeronautical and space activities of the United States shall be conducted so as to contribute . . . to the expansion of human knowledge of phenomena in the atmosphere and space. The Administration shall provide for the widest practicable and appropriate dissemination of information concerning its activities and the results thereof."*

—NATIONAL AERONAUTICS AND SPACE ACT OF 1958

## NASA SCIENTIFIC AND TECHNICAL PUBLICATIONS

**TECHNICAL REPORTS:** Scientific and technical information considered important, complete, and a lasting contribution to existing knowledge.

**TECHNICAL NOTES:** Information less broad in scope but nevertheless of importance as a contribution to existing knowledge.

**TECHNICAL MEMORANDUMS:** Information receiving limited distribution because of preliminary data, security classification, or other reasons.

**CONTRACTOR REPORTS:** Scientific and technical information generated under a NASA contract or grant and considered an important contribution to existing knowledge.

**TECHNICAL TRANSLATIONS:** Information published in a foreign language considered to merit NASA distribution in English.

**SPECIAL PUBLICATIONS:** Information derived from or of value to NASA activities. Publications include conference proceedings, monographs, data compilations, handbooks, sourcebooks, and special bibliographies.

**TECHNOLOGY UTILIZATION PUBLICATIONS:** Information on technology used by NASA that may be of particular interest in commercial and other non-aerospace applications. Publications include Tech Briefs, Technology Utilization Reports and Notes, and Technology Surveys.

*Details on the availability of these publications may be obtained from:*

SCIENTIFIC AND TECHNICAL INFORMATION DIVISION  
NATIONAL AERONAUTICS AND SPACE ADMINISTRATION

Washington, D.C. 20546